

EDCC 127

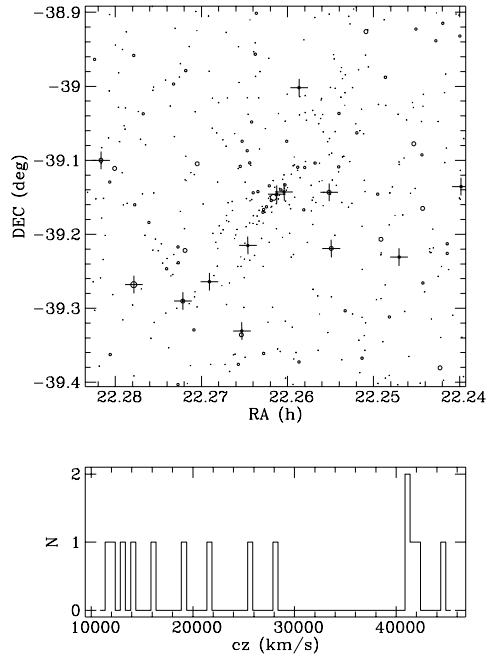


Figure 2. a

EDCC 460

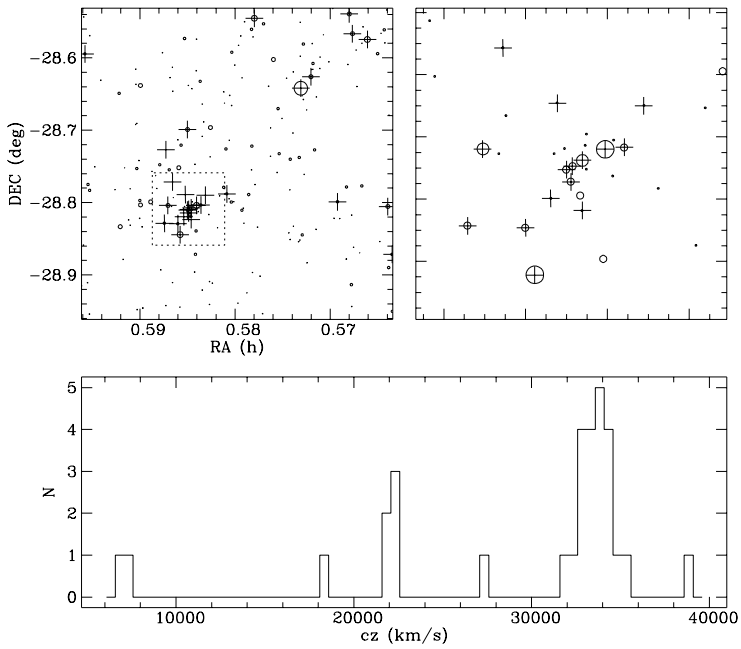


Figure 2. b

EDCC 495

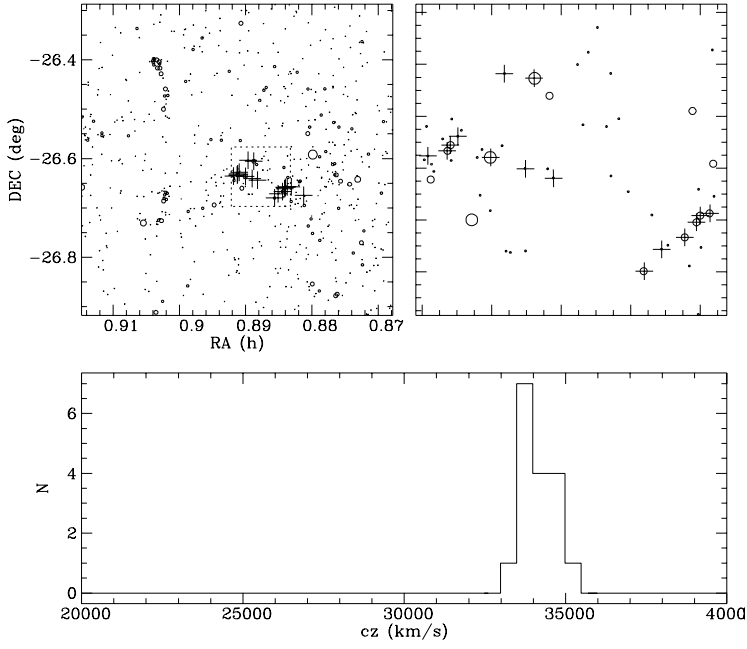


Figure 2. c

EDCC 712

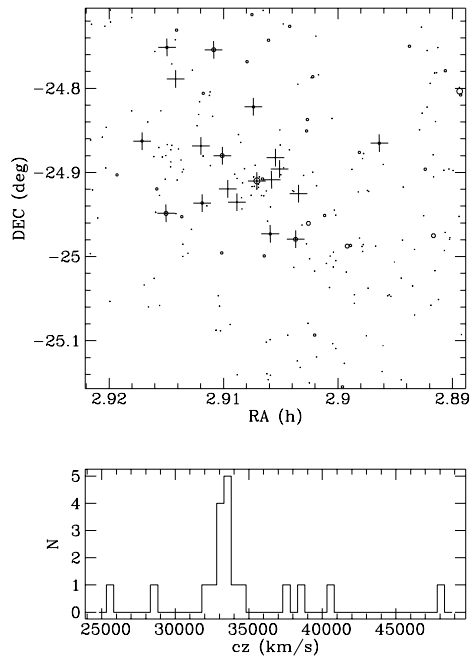


Figure 2. d

EDCC	RA	DEC	$b_j$	$cz_1$	Tel.	$cz_2$	Tel.	$ \Delta v $
235	22 59 54.3	-33 37 11	17.00	26222	ESO 3.6m	26508	ESO 3.6m	286
311	23 28 38.4	-36 44 49	19.22	28588	ESO 3.6m	28595	ESO 3.6m	7
326	23 35 49.9	-38 29 55	18.94	32770	ESO 3.6m	32875	ESO 2.2m	105
326	23 35 57.2	-38 30 36	18.15	19597	ESO 3.6m	18431	ESO 2.2m	1166
348	23 44 53.2	-28 23 11	14.22	7989	ESO 2.2m	7962	AAT	27
348	23 45 07.9	-28 25 01	13.82	8579	ESO 2.2m	8496	AAT	83
408	00 07 23.9	-35 57 11	19.51	35218	ESO 3.6m	36573	ESO 3.6m	1355
408	00 07 24.6	-35 57 33	19.09	36599	ESO 3.6m	36606	ESO 3.6m	7
408	00 07 25.7	-35 57 08	18.91	36787	ESO 3.6m	37568	ESO 3.6m	781
408	00 07 25.9	-35 58 38	18.97	37129	ESO 3.6m	36965	ESO 3.6m	164
410	00 08 49.2	-29 07 58	15.03	18269	ESO 3.6m	18284	ESO 2.2m	15
448	00 26 21.5	-30 22 29	17.82	30752	ESO 3.6m	30982	ESO 3.6m	230
460	00 35 02.0	-28 48 14	16.91	33707	ESO 3.6m	33398	ESO 3.6m	309
460	00 35 02.0	-28 48 14	16.91	33398	ESO 3.6m	33485	ESO 3.6m	87
460	00 35 02.0	-28 48 14	16.91	33707	ESO 3.6m	33356	AAT	351
460	00 35 04.6	-28 48 27	17.02	33267	ESO 3.6m	33788	AAT	519
460	00 35 09.6	-28 49 45	18.53	34116	ESO 3.6m	35602	ESO 3.6m	1485
460	00 35 13.3	-28 48 14	17.67	18548	ESO 3.6m	18749	ESO 3.6m	201
460	00 35 13.3	-28 48 14	17.67	18548	ESO 3.6m	18476	AAT	72
462	00 34 48.4	-39 25 16	18.70	18707	ESO 3.6m	18983	ESO 3.6m	276
462	00 34 58.8	-39 24 48	17.29	19093	ESO 3.6m	18832	ESO 3.6m	261
462	00 35 00.2	-39 23 34	17.26	19605	ESO 3.6m	19006	ESO 3.6m	599
462	00 35 02.5	-39 24 16	15.82	18863	ESO 3.6m	19015	ESO 3.6m	152
482	00 47 03.5	-29 48 05	18.77	33918	ESO 3.6m	33125	AAT	793
571	01 30 03.4	-31 20 57	15.65	21372	ESO 2.2m	21336	ESO 3.6m	36
606	01 58 29.3	-33 13 36	18.72	28771	ESO 3.6m	28510	ESO 3.6m	261
712	02 54 24.8	-24 54 36	16.35	32936	ESO 2.2m	33133	AAT	197
658	02 27 49.0	-33 23 57	16.28	23868	ESO 2.2m	23827	AAT	41
735	03 09 16.4	-27 07 10	15.96	20475	ESO 3.6m	20412	ESO 3.6m	63
742	03 11 48.8	-38 29 11	15.21	25930	ESO 3.6m	25611	ESO 2.2m	319
758	03 20 30.5	-41 31 31	18.34	19387	ESO 3.6m	19390	ESO 3.6m	3

Table 2: Results for galaxies in the survey with two independent observations either at the ESO 3.6 m and 2.2 m telescopes or the AAT. Radial velocities in columns 5 and 7 are heliocentric, in units of  $\text{km s}^{-1}$ .

Table 3

EDCC	RA	DEC	$b_j$	cz	$\Delta$ cz	Notes
5	21 29 11.4	-22 45 35	17.7	33895	114	E
5	21 29 13.6	-22 45 58	19.4	38364	359	E
5	21 29 14.6	-22 47 12	18.8	32735	171	E
5	21 29 14.6	-22 47 37	19.4	33458	120	E
5	21 29 15.2	-22 46 37	17.6	34675	659	E
5	21 29 15.8	-22 48 25	20.4	41266	554	E
42	21 46 23.9	-30 57 04	20.5	35603	125	E
42	21 46 23.3	-30 56 27	18.1	35192	83	E
42	21 46 24.7	-30 57 56	19.1	35189	77	E
42	21 46 30.0	-30 57 28	18.6	35186	137	E
42	21 46 26.2	-30 58 53	18.5	37144	77	E
42	21 46 31.6	-30 59 33	20.3	36265	338	E
42	21 46 26.4	-30 56 47	17.6	36178	56	E
42	21 46 29.2	-30 58 23	19.6	32857	503	E
51	21 49 27.7	-29 06 40	16.4	28159	44	E
51	21 49 25.1	-29 09 32	17.8	27400	41	E
51	21 49 28.4	-29 09 58	17.8	27931	65	E
51	21 49 23.4	-29 00 34	17.0	27673	38	E
51	21 49 26.7	-29 07 29	16.8	27275	32	E
51	21 49 32.6	-29 13 18	16.5	6919	74	E
57	21 54 03.4	-30 20 57	20.3	27553	56	E
57	21 54 13.3	-30 20 00	18.9	27733	38	E
57	21 54 04.0	-30 19 04	17.9	28018	47	E
57	21 53 56.5	-30 19 06	17.5	27706	65	E
80	21 59 03.2	-22 39 09	16.5	21716	71	E
80	21 59 04.5	-22 39 11	16.7	21489	59	E
80	21 59 09.4	-22 38 23	18.0	21947	56	E
80	21 59 15.6	-22 38 13	17.7	21291	56	E
80	21 59 03.7	-22 43 36	14.8	21270	59	E
80	22 59 59.7	-22 42 52	15.0	21108	47	E,AC
80	21 59 01.5	-22 39 46	19.0	20143	56	E
80	21 59 06.1	-22 40 29	15.0	19924	38	E
80	21 59 09.9	-22 39 27	16.1	20502	35	E
80	21 59 08.7	-22 38 38	19.0	20280	65	E
80	21 59 08.9	-22 37 36	17.6	19183	383	E
80	22 00 14.0	-22 57 22	18.6	20460	290	A

EDCC	RA	DEC	$b_j$	cz	$\Delta$ cz	Notes
80	22 00 20.3	-23 02 35	17.8	21956	89	A
80	22 00 23.6	-23 07 14	17.6	20466	62	A
80	22 01 05.2	-23 11 26	17.4	20613	155	A
80	22 00 30.0	-23 08 23	18.4	21042	68	A
80	22 00 08.0	-23 13 33	17.5	21297	89	A
80	21 59 37.5	-23 11 39	16.6	21048	53	A
80	21 59 35.9	-23 09 26	17.2	21564	56	A
80	21 59 43.8	-23 07 56	17.1	20937	100	A
80	21 59 37.8	-23 07 41	17.2	21516	51	A
80	21 59 49.9	-23 01 36	18.1	21830	44	A
80	21 59 40.3	-23 02 23	16.6	19357	35	A
80	21 58 47.7	-22 59 11	16.9	21450	101	A
80	21 58 43.2	-22 56 52	17.7	19177	122	A
80	21 59 10.6	-22 53 46	17.1	21057	98	A
80	21 59 18.9	-22 51 00	18.5	21812	80	A
80	21 59 36.9	-22 46 32	17.0	21791	122	A
80	21 59 47.3	-22 58 00	18.3	22217	251	A
80	21 58 57.4	-23 11 24	17.3	32833	77	A
80	21 59 38.8	-22 56 03	18.8	10189	431	A
80	21 59 58.8	-22 58 32	18.3	32680	104	A
80	22 00 08.9	-22 52 53	18.1	13847	86	A
80	22 00 24.3	-23 03 23	16.8	16200	71	A
80	22 00 44.0	-22 57 40	17.6	22148	57	A
80	22 00 07.4	-22 58 26	17.6	22051	75	A
99	22 06 30.2	-27 33 09	17.8	19105	38	E
99	22 06 32.9	-27 33 00	17.6	19135	41	E
99	22 06 23.1	-27 34 29	17.2	27140	38	E
99	22 06 24.3	-27 33 58	18.9	26507	101	E
114	22 11 08.8	-36 55 44	15.3	10180	68	E
114	22 11 15.4	-36 56 37	16.0	10183	53	E
115	22 10 24.2	-34 54 51	19.0	21821	294	E
115	22 10 34.2	-34 55 01	17.8	21995	56	E
115	22 10 38.7	-34 54 29	18.2	21833	65	E
115	22 10 36.8	-34 54 36	18.2	45229	65	E

EDCC	RA	DEC	$b_j$	cz	$\Delta$ cz	Notes
124	22 14 41.2	-35 58 00	18.0	43511	104	E
124	22 14 42.1	-35 57 57	19.4	42102	38	E
124	22 14 43.4	-35 58 08	20.1	44219	197	E
124	22 14 47.8	-36 00 07	19.7	44489	62	E
124	22 14 57.6	-35 57 57	20.8	45538	95	E,AC
124	22 14 51.6	-35 58 42	18.0	43646	131	E
124	22 14 53.2	-35 58 50	18.3	43643	47	E
124	22 14 54.1	-35 59 17	18.4	44462	77	E
124	22 14 48.2	-35 58 07	19.0	48104	47	E
124	22 14 55.5	-35 57 58	20.1	46066	65	E,AC
127	22 15 40.5	-39 08 45	18.5	41949	56	A
127	22 15 52.6	-39 12 54	18.0	41431	89	A
127	22 15 37.4	-39 08 34	18.9	41032	122	A
127	22 15 31.1	-39 00 07	18.8	41077	140	A,AC
127	22 16 54.0	-39 06 00	17.5	11985	41	A
127	22 15 55.1	-39 19 50	18.0	13229	95	A
127	22 15 18.6	-39 08 36	17.3	14237	83	A
127	22 14 23.4	-39 08 08	18.2	11880	321	A
127	22 15 17.7	-39 13 09	17.7	16347	71	A
127	22 14 49.3	-39 13 51	18.8	21498	311	A
127	22 14 07.5	-39 00 37	18.4	19096	307	A
127	22 16 40.3	-39 16 05	17.0	25422	59	A
127	22 16 19.8	-39 17 25	17.1	28261	131	A
127	22 16 08.7	-39 15 51	18.4	44845	86	A
131	22 17 06.0	-34 51 02	17.9	47493	104	E
131	22 16 46.2	-34 50 02	17.5	46749	26	E,AC
131	22 16 57.8	-34 49 57	18.4	47058	53	E
131	22 17 07.8	-34 52 19	18.0	46230	62	E
145	22 25 01.0	-30 49 04	17.1	16788	50	A
145	22 25 05.2	-30 48 55	17.3	18934	50	A
145	22 26 04.5	-30 53 06	17.8	17876	53	A
145	22 25 30.3	-30 53 34	17.3	16974	65	A
145	22 25 44.4	-30 56 20	17.8	17118	56	A
145	22 25 16.1	-30 52 47	17.0	15382	134	A
145	22 25 03.9	-30 53 16	17.2	17807	56	A
145	22 25 18.4	-31 01 15	17.6	16659	44	A
145	22 25 07.0	-30 57 15	16.5	17672	59	A

EDCC	RA	DEC	$b_j$	cz	$\Delta$ cz	Notes
145	22 24 56.0	-30 59 28	16.7	14767	59	A
145	22 24 34.2	-30 45 03	16.2	17576	107	A
145	22 25 28.1	-30 40 58	18.1	7701	38	A
172	22 36 15.4	-36 51 06	16.2	17070	32	E
172	22 35 44.0	-37 01 33	17.3	17501	38	E
172	22 35 54.1	-37 00 18	15.8	18050	38	E
172	22 36 04.6	-36 53 16	16.7	23209	47	E
175	22 36 47.4	-38 07 06	17.9	46123	41	E
175	22 36 44.5	-38 07 18	18.1	46284	32	E
175	22 36 59.8	-38 05 56	17.6	45682	38	E
175	22 35 55.3	-38 05 19	18.3	56915	38	E
178	-	-	-	14824	68	E,NC
178	-	-	-	14983	38	E,NC
198	22 46 35.1	-41 10 48	18.6	37989	41	E
198	22 46 33.0	-41 10 33	18.7	37536	47	E
198	22 46 37.5	-41 09 27	18.8	37863	35	E
198	22 46 23.1	-41 10 52	19.1	57188	38	E
198	22 46 22.0	-41 11 04	19.2	58129	59	E
198	22 46 43.2	-41 07 39	19.4	62887	98	E
201	22 46 48.4	-31 32 00	17.2	31202	26	E
201	22 46 48.8	-31 30 57	17.6	32026	29	E
201	22 47 10.8	-31 23 59	18.1	34598	47	E
201	22 47 17.6	-31 23 30	17.1	33891	35	E
216	22 50 48.2	-25 49 20	16.9	23269	29	E
216	22 50 54.7	-25 47 29	19.9	25869	59	E
216	22 50 46.4	-25 49 03	18.7	26978	56	E
216	22 50 50.6	-25 48 45	20.6	46773	50	E
216	22 50 51.3	-25 48 16	20.0	45439	38	E
230	22 55 59.9	-31 08 29	17.8	33525	41	E
230	22 55 58.5	-31 09 02	18.3	32302	32	E
230	22 55 34.4	-31 07 01	17.2	24391	65	E
230	22 55 37.3	-31 06 50	18.3	37821	47	E

EDCC	RA	DEC	$b_j$	cz	$\Delta$ cz	Notes
235	22 59 49.4	-33 37 09	18.6	26183	80	E
235	22 59 54.3	-33 37 11	17.2	26222	35	E
235	22 59 49.3	-33 36 27	19.4	19354	137	E
235	23 00 06.9	-33 39 32	17.2	19720	26	E
247	23 02 59.4	-39 21 03	18.4	49840	53	E
247	23 02 55.0	-39 21 38	18.1	49720	56	E
247	23 02 58.0	-39 20 08	18.7	26408	41	E
247	23 02 58.1	-39 18 50	18.4	50781	44	E
256	23 07 52.8	-23 12 20	18.3	27359	32	E
256	23 07 46.2	-23 12 06	17.9	27143	26	E
256	23 07 50.6	-23 18 39	18.1	32824	32	E
256	23 07 58.0	-23 17 44	18.0	33079	29	E
261	23 08 59.1	-29 22 03	17.4	25842	41	E
261	23 08 53.3	-29 21 32	17.8	25893	26	E
261	23 09 01.9	-29 23 34	18.1	36640	29	E
261	23 08 57.4	-29 22 58	17.1	35036	80	E
261	23 08 56.0	-29 21 41	18.4	36697	95	E
261	-	-	-	34344	71	E,NC
261	-	-	-	35588	56	E,NC
261	-	-	-	35381	65	E,NC
269	23 11 47.9	-38 01 44	18.3	28150	47	A
269	23 11 33.8	-38 00 00	17.7	28021	29	A
269	23 12 13.6	-38 02 00	18.6	27574	59	A
269	23 12 05.4	-38 00 26	17.0	28105	74	A
269	23 11 40.6	-37 49 39	18.0	28225	38	A
269	23 13 53.8	-38 12 19	17.6	18898	38	A
269	23 12 57.1	-38 12 04	17.6	20092	35	A
269	23 12 10.2	-38 19 45	17.0	18137	29	A
269	23 11 52.5	-37 58 10	19.0	20274	83	A
269	23 12 52.9	-38 00 10	18.0	53635	83	A
269	23 13 01.9	-38 04 09	17.9	53321	29	A
269	23 12 18.0	-38 03 17	19.0	55497	74	A
285	23 17 49.4	-42 03 53	17.9	17133	29	E
285	23 17 49.2	-42 04 30	17.0	16518	35	E,AC
285	23 19 08.3	-42 10 47	17.7	26090	41	E
285	23 18 56.6	-42 10 12	16.0	26933	44	E,AC

EDCC	RA	DEC	$b_j$	cz	$\Delta$ cz	Notes
297	23 24 05.8	-24 09 36	18.9	26642	74	E
297	23 23 55.8	-24 08 38	19.0	27113	44	E
297	23 24 03.1	-24 07 45	17.2	26498	35	E
297	23 24 08.4	-24 09 15	19.9	32971	419	E
297	23 23 53.3	-24 09 09	19.8	35240	68	E
307	23 26 58.9	-39 41 51	16.9	16188	47	E
307	23 27 19.6	-39 37 11	17.1	15945	32	E
307	23 27 15.5	-39 43 39	17.1	16968	38	E
311	23 28 36.4	-36 47 15	19.7	28819	35	E
311	23 28 38.4	-36 44 49	19.2	28588	119	E
311	23 28 41.1	-36 46 42	19.2	28579	38	E
311	23 28 45.6	-36 46 16	17.9	28486	161	E
311	23 28 31.4	-36 47 29	18.6	30311	86	E
311	23 28 37.2	-36 47 07	18.2	29664	98	E
311	23 28 44.0	-36 45 33	20.2	26957	41	E
316	23 30 07.8	-36 28 01	18.2	27940	47	E
316	23 30 10.1	-36 31 05	17.9	28270	35	E
316	23 30 11.1	-36 30 28	17.3	28549	41	E
316	23 30 08.1	-36 28 58	17.2	28672	47	E
326	23 35 43.9	-38 29 45	18.8	32389	59	E
326	23 35 49.2	-38 31 27	19.2	32590	35	E
326	23 35 49.9	-38 29 55	18.9	32770	53	E
326	23 35 57.5	-38 30 36	18.2	18431	59	E
326	23 35 49.9	-38 30 08	20.0	49531	104	E,AC
326	23 35 53.6	-38 30 08	18.9	49702	68	E
326	23 35 57.5	-38 30 11	19.6	71155	59	E
332	23 38 58.4	-29 30 50	15.5	15217	44	E
332	23 38 44.2	-29 25 52	18.9	15661	83	E
332	23 38 52.8	-29 35 53	15.1	15670	38	E
348	23 45 09.9	-28 23 08	18.2	8064	26	A
348	23 46 08.0	-28 25 17	14.8	7791	89	A,AC
348	23 45 45.3	-28 23 39	16.0	8864	26	A
348	23 45 23.1	-28 25 11	16.7	7359	14	A
348	23 45 50.4	-28 33 24	16.6	8130	20	A

EDCC	RA	DEC	$b_j$	$cz$	$\Delta cz$	Notes
348	23 45 18.3	-28 26 36	17.5	9002	14	A
348	23 45 13.5	-28 34 09	18.1	8864	23	A
348	23 45 06.8	-28 27 04	18.3	8241	26	A,AC
348	23 44 53.2	-28 23 11	14.1	7962	32	A
348	23 44 35.4	-28 31 06	18.3	7701	29	A
348	23 45 06.8	-28 26 04	18.3	7911	29	A
348	23 44 38.4	-28 28 15	17.0	8756	20	A
348	23 45 07.9	-28 25 01	13.8	8496	23	A
348	23 44 40.9	-28 24 07	16.7	8804	20	A
348	23 44 59.6	-28 24 12	17.1	9185	17	A
348	23 44 53.2	-28 23 11	14.1	8112	86	A
348	23 45 04.0	-28 22 52	18.4	9161	23	A
348	23 44 44.2	-28 20 27	17.4	8295	29	A
348	23 44 38.5	-28 18 29	18.9	8223	44	A
348	23 44 54.7	-28 19 16	17.6	8163	29	A
348	23 44 46.0	-28 15 12	17.1	7317	14	A
348	23 45 03.5	-28 17 26	17.5	7833	23	A
348	23 45 23.1	-28 25 11	16.7	9596	14	A
348	23 45 43.3	-28 27 25	16.8	10486	20	A
348	23 45 25.5	-28 26 28	18.1	9599	20	A
348	23 45 13.7	-28 28 54	17.4	9545	17	A
348	23 45 14.5	-28 25 49	17.8	9773	29	A
348	23 44 52.2	-28 32 59	17.4	10102	29	A
348	23 44 58.8	-28 25 56	18.0	9599	20	A
348	23 44 47.3	-28 23 49	16.5	9647	17	A
348	23 44 37.4	-28 17 42	17.0	9971	23	A
348	23 43 04.5	-28 16 47	18.1	9641	29	A
348	23 44 37.4	-28 29 27	18.4	18940	26	A
366	23 52 11.5	-27 58 04	19.1	22580	80	E
366	23 52 10.8	-27 57 35	16.9	21836	47	E
366	23 52 10.9	-27 56 34	18.2	21686	53	E
366	23 52 10.7	-27 56 22	18.2	20499	332	E
366	23 52 12.7	-27 55 54	17.8	21426	74	E
366	23 52 14.5	-27 55 50	17.8	22016	29	E
366	23 52 14.5	-27 55 26	18.4	22691	65	E
366	23 52 18.8	-27 57 34	18.4	15760	95	E
372	23 54 26.0	-34 57 32	14.7	12675	35	E

EDCC	RA	DEC	$b_j$	$cz$	$\Delta cz$	Notes
392	00 00 02.4	-34 58 45	19.2	33888	295	E
392	00 00 03.8	-34 58 02	19.5	34419	71	E
392	00 00 12.4	-34 57 21	18.0	33402	62	E
392	00 00 10.7	-34 55 37	18.7	33327	53	E
392	00 00 16.5	-34 56 15	18.5	33927	53	E
392	00 00 06.4	-34 58 18	19.0	33127	56	E
392	00 00 10.5	-34 57 19	18.2	32650	41	E
392	00 00 13.3	-34 58 25	18.1	35873	41	E
394	00 00 07.4	-36 12 51	17.8	14950	59	E
394	00 00 10.5	-36 12 28	17.8	14668	29	E
394	00 00 15.6	-36 11 44	18.2	14431	38	E
394	00 00 39.5	-36 12 55	14.6	14728	47	E
394	00 00 11.6	-36 12 31	19.1	13808	56	E
394	00 00 17.2	-36 12 07	18.9	15724	77	E
400	00 03 39.1	-34 59 45	19.4	34077	107	E
400	00 03 43.3	-34 59 06	19.3	32452	80	E
400	00 03 46.4	-34 57 34	19.0	35453	92	E
400	00 03 42.7	-34 56 32	20.4	34619	119	E
400	00 03 44.6	-34 56 52	19.9	32878	146	E
400	00 03 41.8	-34 59 19	19.2	17151	71	E
400	00 03 42.8	-34 57 51	18.3	35987	44	E
400	00 03 43.2	-34 58 30	18.5	17765	86	E
400	00 03 46.0	-35 00 32	19.0	86762	68	E
400	00 03 46.8	-34 58 01	19.4	35576	146	E
408	00 07 23.9	-35 57 11	19.5	36573	143	E
408	00 07 25.0	-35 57 20	20.5	35069	113	E,AC
408	00 07 26.0	-35 56 49	21.	34784	53	E,AC
408	00 07 26.8	-35 56 33	17.4	35107	113	E
408	00 07 23.0	-38 58 30	20.0	36058	74	E,AC
408	00 07 28.2	-35 56 52	19.3	35492	83	E
408	00 07 28.9	-35 56 41	17.9	34281	89	E
408	00 07 30.0	-35 56 30	19.5	34748	74	E,AC
408	00 07 25.9	-35 58 38	19.0	37129	50	E
408	00 07 25.7	-35 57 08	18.9	36787	74	E
408	00 07 24.6	-35 57 33	19.1	36606	50	E
408	00 07 25.7	-35 57 08	18.9	36736	50	E
408	00 07 21.0	-35 58 23	19.4	36841	53	E
408	00 07 24.9	-35 57 14	19.7	37767	374	E



EDCC	RA	DEC	$b_j$	$cz$	$\Delta cz$	Notes
410	00 08 49.5	-29 07 58	15.0	18269	32	E
410	00 09 11.6	-29 12 37	16.0	18617	29	E
418	00 13 11.6	-23 58 42	17.1	19234	80	A
418	00 13 31.2	-24 01 52	17.0	20361	53	A
418	00 13 26.0	-24 04 12	16.7	18997	56	A
418	00 13 33.2	-24 00 29	16.4	20370	49	A
418	00 12 35.0	-24 22 23	15.7	19846	56	A
418	00 12 08.0	-24 17 49	16.9	20811	62	A
418	00 12 46.5	-24 08 18	17.4	19420	53	A
418	00 12 06.1	-24 01 15	17.3	18671	71	A
418	00 12 37.0	-24 00 34	17.9	48011	53	A
419	00 12 31.2	-26 32 14	18.1	39026	38	A
419	00 12 46.1	-26 19 09	18.5	36832	35	A
419	00 11 38.3	-26 27 24	17.7	25964	38	A
419	00 12 38.1	-26 22 46	18.1	35786	74	A
419	00 12 50.0	-26 21 07	17.8	43499	56	A,AC
421	00 13 38.8	-35 10 19	19.7	45184	128	E
421	00 13 39.7	-35 10 23	18.0	45034	26	E
421	00 13 40.5	-35 11 12	19.6	42411	170	E
421	00 13 38.6	-35 12 15	19.9	42462	86	E
421	00 13 41.2	-35 12 19	18.2	44024	68	E
421	00 13 30.3	-35 09 59	19.4	29193	38	E
421	00 13 39.0	-35 09 48	20.0	96281	575	E,AC
424	-	-	-	22340	26	E,NC
424	-	-	-	22916	47	E,NC
429	00 15 05.6	-35 27 28	18.5	29595	59	E
429	00 15 04.4	-35 27 40	16.8	28573	89	E
429	00 15 01.4	-35 28 35	17.8	29523	38	E
429	00 15 09.2	-35 27 51	19.1	27706	83	E
429	00 15 02.1	-35 29 06	18.4	29613	56	E
429	00 15 05.7	-35 28 49	18.0	28878	62	E
429	00 15 07.5	-35 28 39	19.0	29550	188	E
429	00 15 15.0	-35 29 11	19.0	30488	56	E
429	00 15 05.4	-35 29 20	18.6	27460	56	E
429	00 15 10.3	-35 28 40	16.8	28753	179	E

EDCC	RA	DEC	$b_j$	$cz$	$\Delta cz$	Notes
429	00 15 05.2	-35 29 39	18.1	28872	44	E
429	00 15 11.6	-35 28 47	18.4	27377	62	E
429	00 15 06.1	-35 29 50	17.3	29328	47	E
429	00 15 05.7	-35 30 04	18.5	29208	53	E
429	00 15 16.4	-35 25 56	18.1	29403	53	E
429	00 15 08.1	-35 30 25	18.9	29997	35	E
429	00 15 10.4	-35 30 30	19.3	29676	80	E
429	00 15 08.3	-35 27 46	20.3	19333	44	E
429	00 15 10.0	-35 29 46	19.3	36382	59	E
437	00 18 14.7	-25 45 27	18.0	19936	179	A
437	00 18 11.4	-25 49 28	17.9	19258	50	A
437	00 17 35.2	-26 00 24	17.9	19429	53	A
437	00 17 56.0	-25 51 33	18.0	17417	313	A
437	00 17 21.0	-25 53 43	17.9	18943	35	A
437	00 17 06.4	-25 54 59	17.5	33756	86	A
438	00 20 14.9	-38 23 38	17.9	35711	83	E
438	00 20 16.8	-38 23 30	17.1	35750	44	E
438	00 20 11.5	-38 24 09	18.5	36838	101	E
438	00 20 12.6	-38 24 02	18.6	34883	44	E
447	00 26 06.9	-23 55 25	19.1	33216	71	E,AC
447	00 26 06.5	-23 54 56	17.8	33564	26	E,AC
447	00 26 08.5	-23 52 36	17.6	34371	26	E
447	00 26 11.2	-23 52 49	18.1	34239	38	E
447	00 26 02.0	-23 54 47	18.7	58069	35	E
447	00 26 09.4	-23 54 34	19.2	31819	29	E
448	00 26 14.8	-30 23 24	19.2	30515	68	E
448	00 26 17.6	-30 22 58	19.4	30258	41	E
448	00 26 18.7	-30 23 06	19.3	31235	140	E
448	00 26 20.5	-30 23 01	20.1	32506	116	E
448	00 26 21.5	-30 22 29	17.8	30752	38	E
448	00 26 27.5	-30 22 20	19.5	30809	74	E
448	00 26 28.7	-30 21 39	18.0	30638	71	E,AC
448	00 26 29.0	-30 21 40	18.0	30962	29	E,AC
448	00 25 50.2	-30 31 20	18.6	32884	92	E
448	00 25 55.0	-30 31 11	18.6	31178	83	E
448	00 26 17.1	-30 22 23	18.5	38394	38	E

EDCC	RA	DEC	$b_j$	cz	$\Delta cz$	Notes
448	00 26 18.4	-30 22 54	19.0	38139	38	E
448	00 26 19.3	-30 22 42	18.8	38715	56	E
448	00 26 22.4	-30 21 08	18.6	35477	44	E
448	00 25 46.8	-30 31 12	18.5	36244	41	E
448	00 25 48.3	-30 32 13	18.9	36103	65	E
448	00 25 44.5	-30 29 11	16.8	21333	65	E
450	00 27 12.8	-29 42 53	18.0	30671	44	E
450	00 27 17.8	-29 41 34	18.7	30225	44	E
450	00 27 19.0	-29 41 26	18.0	28690	44	E
450	00 27 24.7	-29 42 01	18.3	28947	32	E
450	00 27 19.4	-29 41 00	20.9	38679	41	E,AC
460	00 35 00.9	-28 48 12	18.6	32473	86	E
460	00 35 14.2	-28 43 37	19.6	33393	137	E
460	00 35 04.6	-28 48 27	17.0	33267	41	E
460	00 35 06.0	-28 48 38	18.0	32989	59	E
460	00 35 09.6	-28 49 45	18.5	34116	32	E
460	00 34 59.2	-28 47 24	20.1	34850	200	E
460	00 35 04.6	-28 49 25	20.5	38730	68	E
460	00 35 05.5	-28 48 34	18.4	32680	128	E
460	00 35 07.4	-28 49 11	19.3	31984	59	E
460	00 35 13.4	-28 48 14	17.7	18548	53	E
460	00 35 05.6	-28 48 52	18.2	34023	35	E
460	00 35 06.8	-28 47 21	19.7	32764	74	E
460	00 35 11.6	-28 46 17	19.1	35120	158	E
460	00 35 14.7	-28 49 43	18.9	34212	83	E
460	00 35 06.0	-28 41 57	17.4	34308	56	A
460	00 35 02.6	-28 48 14	16.8	33354	53	A
460	00 35 08.8	-28 50 40	17.9	34074	53	A
460	00 34 51.1	-28 47 17	18.6	34095	26	A
460	00 34 09.2	-28 47 56	18.6	33852	50	A
460	00 33 35.0	-28 52 04	18.2	33897	47	A
460	00 33 50.2	-28 48 20	17.9	33043	38	A
460	00 33 28.4	-28 31 40	18.1	33552	53	A
460	00 34 19.3	-28 37 34	17.3	33756	41	A
460	00 33 40.6	-28 36 02	18.5	7090	68	A
460	00 33 48.6	-28 52 17	18.4	27409	47	A
460	00 33 57.9	-28 34 29	16.1	22208	50	A
460	00 34 03.6	-28 34 00	17.0	22250	47	A

EDCC	RA	DEC	$b_j$	cz	$\Delta cz$	Notes
460	00 34 04.8	-28 32 21	17.9	22241	32	A
460	00 34 23.1	-28 38 31	14.2	7108	17	A
460	00 34 40.7	-28 32 43	16.6	21785	56	A
460	00 35 44.8	-28 35 40	18.6	21785	26	A
462	00 34 48.2	-39 25 16	18.7	18707	56	E
462	00 34 56.7	-39 25 43	19.4	18671	62	E
462	00 34 57.4	-39 25 35	18.9	17858	35	E
462	00 34 59.1	-39 25 18	18.3	17807	23	E
462	00 34 52.7	-39 24 34	18.5	19675	239	E
462	00 34 59.0	-39 24 48	17.3	18832	23	E
462	00 35 02.5	-39 24 16	15.8	19015	26	E
462	00 34 59.9	-39 23 44	17.8	19669	29	E
462	00 35 00.2	-39 23 34	17.3	19006	482	E
462	00 35 00.0	-39 24 43	19.0	33999	104	E
462	00 34 46.3	-39 27 17	17.0	19069	29	E
462	00 34 54.9	-39 25 53	19.0	19180	41	E
470	00 37 16.7	-26 29 55	18.2	33408	44	E
470	00 37 17.7	-26 29 57	18.7	32491	26	E
470	00 37 20.9	-26 29 13	18.8	33600	110	E,AC
470	00 37 22.6	-26 27 37	17.3	32896	68	E
470	00 37 24.3	-26 28 23	20.0	32518	74	E
470	00 37 27.0	-26 29 11	16.9	32968	29	E
470	00 37 27.4	-26 30 14	19.5	32428	104	E
470	00 37 18.5	-26 30 13	18.1	31987	26	E
470	00 37 22.1	-26 30 32	19.9	34479	44	E
470	00 37 25.7	-26 29 09	18.9	35105	38	E
471	00 37 49.8	-24 57 43	20.3	33513	131	E
471	00 37 52.9	-24 59 00	18.6	33264	86	E
471	00 37 54.9	-24 59 27	18.2	33684	47	E
471	00 37 55.5	-25 00 12	18.4	33261	53	E
471	00 37 56.5	-24 58 34	19.2	33861	50	E
471	00 37 58.7	-24 59 14	19.2	31433	74	E
471	00 38 01.2	-25 00 17	18.2	34733	59	E
473	00 39 33.7	-28 49 16	19.1	33112	50	E
473	00 39 31.6	-28 47 34	18.6	32548	128	E
473	00 39 35.0	-28 48 00	18.6	31322	35	E

EDCC	RA	DEC	$b_j$	cz	$\Delta$ cz	Notes
473	00 39 37.2	-28 48 26	18.1	31340	26	E
473	00 39 44.3	-28 50 31	19.6	32218	44	E
473	00 39 41.5	-28 48 35	16.1	32434	23	E
473	00 39 44.5	-28 49 01	18.8	32818	44	E
473	00 39 46.4	-28 49 26	19.0	31984	29	E
473	00 39 37.4	-28 49 48	19.5	29274	95	E
473	00 39 44.3	-28 47 35	18.0	33162	23	E
473	00 39 47.6	-28 49 22	20.0	34194	56	E
473	-	-	-	32794	26	E,NC
473	-	-	-	32482	29	E,NC
473	-	-	-	33076	32	E,NC
474	00 40 20.5	-26 20 06	18.7	34359	29	E
474	00 40 22.9	-26 21 11	17.2	32896	23	E
474	00 40 25.0	-26 21 02	19.3	33771	38	E
474	00 40 26.4	-26 23 11	17.8	33807	38	E
474	00 40 27.8	-26 21 27	17.5	33753	23	E
474	00 40 28.6	-26 22 10	18.7	33774	56	E
474	00 40 24.5	-26 20 58	19.6	33801	38	E
474	00 40 31.0	-26 21 36	18.8	33795	68	E
474	00 40 32.1	-26 21 53	18.8	30045	83	E
474	00 40 33.2	-26 23 10	19.6	30272	32	E
474	00 41 09.6	-26 14 01	17.8	16308	56	E
474	00 41 16.0	-26 14 16	16.7	16362	35	E
474	00 41 17.7	-26 17 05	17.4	30063	47	E
474	00 41 21.9	-26 17 20	17.3	16224	35	E
474	00 41 28.7	-26 17 42	19.3	36706	53	E
482	00 46 48.4	-28 46 51	20.0	31022	53	E,AC
482	00 46 58.8	-29 47 56	18.0	32278	29	E
482	00 46 58.8	-29 47 56	18.0	32476	77	E,AC
482	00 46 58.1	-29 47 33	17.2	31454	38	E
482	00 47 00.4	-29 46 24	19.9	32839	23	E
482	00 47 00.2	-29 46 24	18.0	31819	98	E,AC
482	00 47 03.4	-29 48 05	18.8	33918	41	E
482	00 47 05.3	-29 47 17	18.5	32812	29	E,AC
482	00 46 48.4	-28 46 51	20.0	64910	29	E,AC
482	00 46 56.0	-29 47 56	19.6	48641	44	E
482	00 46 54.4	-29 44 56	18.2	32329	65	A
482	00 46 51.4	-29 46 47	18.5	32353	47	A

EDCC	RA	DEC	$b_j$	cz	$\Delta$ cz	Notes
482	00 46 59.2	-29 47 44	18.0	32578	41	A
482	00 47 04.3	-29 45 49	18.0	34068	32	A
482	00 47 17.0	-29 50 36	17.9	32548	41	A
482	00 47 32.2	-29 52 27	18.0	32290	29	A
482	00 47 03.0	-29 50 29	18.3	32047	53	A
482	00 47 26.2	-29 51 50	17.1	33162	83	A
482	00 46 53.9	-29 49 24	18.7	32716	38	A
482	00 46 38.4	-29 52 20	18.3	32476	47	A
482	00 46 29.5	-29 57 22	18.1	32119	26	A
482	00 46 31.3	-29 44 09	18.9	31897	44	A
482	00 46 40.1	-29 42 52	18.6	31436	62	A
482	00 45 53.4	-29 44 20	17.9	23018	89	A
482	00 45 59.5	-29 45 11	18.3	22457	44	A
482	00 46 31.5	-29 47 25	18.4	22511	59	A
482	00 46 33.3	-29 53 47	17.4	22742	41	A
482	00 46 45.8	-29 41 23	17.6	22820	32	A
482	00 46 56.5	-29 51 15	18.4	22697	71	A
482	00 47 12.7	-29 56 57	18.7	22706	26	A
485	00 48 49.7	-28 47 51	17.5	33309	44	E
485	00 48 58.5	-28 46 09	16.7	32956	50	E
485	00 49 00.8	-28 46 35	18.1	33813	50	E
485	00 48 56.9	-28 47 57	16.6	33981	26	E
485	00 48 44.6	-28 46 16	17.2	34170	26	E
485	00 48 43.2	-28 45 38	17.3	34152	74	E
494	00 53 11.8	-37 32 10	17.2	17058	44	E
494	00 53 24.8	-37 33 43	16.8	16455	35	E
494	00 53 24.0	-37 35 22	16.5	16866	44	E,AC
494	00 53 24.1	-37 40 44	15.4	16563	47	E
495	00 52 52.4	-26 40 28	19.3	34173	23	E
495	00 53 01.4	-26 39 27	18.9	33924	26	E
495	00 53 02.8	-26 39 39	18.5	33900	35	E
495	00 53 04.0	-26 40 00	18.1	33483	26	E
495	00 52 59.1	-26 39 27	20.1	33816	32	E
495	00 53 06.4	-26 40 17	19.0	33996	23	E
495	00 53 08.2	-26 40 47	18.5	33696	53	E
495	00 53 19.6	-26 36 19	17.4	35084	59	E
495	00 53 22.7	-26 36 13	19.7	34395	68	E

EDCC	RA	DEC	$b_j$	cz	$\Delta cz$	Notes
495	00 53 17.6	-26 38 38	19.6	34643	71	E
495	00 53 20.5	-26 38 25	19.4	34712	44	E
495	00 53 24.1	-26 38 09	17.3	34730	35	E
495	00 53 27.5	-26 37 40	19.6	34275	35	E
495	00 53 28.3	-26 37 52	18.3	33894	50	E
495	00 53 02.4	-26 39 30	18.3	34494	104	E
495	00 53 28.6	-26 38 00	18.9	33816	29	E
495	00 53 30.6	-26 38 07	19.2	33720	74	E
499	00 53 39.4	-38 10 26	16.6	35261	59	E
499	00 53 44.5	-38 09 53	18.2	34973	44	E
499	00 53 26.5	-38 12 41	18.1	34967	35	E
499	00 53 34.9	-38 13 15	17.7	34302	44	E
500	00 54 03.4	-30 19 37	18.6	33813	71	E
500	00 54 08.3	-30 20 42	17.8	33984	53	E
500	00 54 13.6	-30 19 38	18.2	34011	50	E
500	00 54 03.2	-30 18 25	18.9	28675	56	E
500	00 54 05.9	-30 22 02	18.2	47370	26	E
500	00 54 05.7	-30 22 40	19.0	49705	50	E
500	00 54 09.8	-30 18 47	20.5	64374	50	E,AC
519	01 02 34.7	-40 01 45	17.8	31939	50	A
519	01 03 35.0	-40 07 08	18.1	31616	62	A
519	01 03 02.5	-40 10 56	17.7	31703	71	A
519	01 02 17.2	-40 13 51	18.3	31951	50	A
519	01 02 07.5	-40 10 48	18.1	32437	50	A
519	01 02 03.8	-40 06 56	17.5	32761	110	A
519	01 01 45.7	-40 03 04	16.6	31975	152	A
519	01 01 56.2	-40 02 45	17.8	32659	59	A
519	01 01 50.1	-40 01 20	18.4	31858	41	A
519	01 01 03.0	-40 07 20	17.1	28279	83	A
519	01 01 21.1	-40 08 46	16.5	9062	14	A
519	01 02 15.0	-40 22 20	17.5	27838	41	A
519	01 02 52.2	-40 10 45	17.9	27499	32	A
520	01 02 01.7	-24 13 41	20.3	48302	59	E
520	01 02 02.0	-24 13 26	19.3	49852	35	E
520	01 02 04.0	-24 14 06	20.4	48908	53	E
520	01 02 04.4	-24 13 37	19.2	47735	38	E

EDCC	RA	DEC	$b_j$	cz	$\Delta cz$	Notes
520	01 02 06.7	-24 13 52	19.5	46935	50	E,AC
520	01 02 07.3	-24 15 50	18.9	46929	29	E
520	01 02 08.3	-24 14 32	17.3	47843	29	E
520	01 02 11.6	-24 13 52	20.8	47960	89	E
520	01 02 06.6	-24 15 53	19.2	56357	74	E
520	01 02 13.2	-24 13 38	18.6	34539	104	E
520	01 02 14.3	-24 13 56	20.6	57383	41	E
524	01 05 40.7	-36 59 59	18.4	33960	147	E
524	01 05 45.0	-37 03 23	19.6	35555	65	E
524	01 05 47.1	-37 03 20	18.3	34266	41	E
524	01 05 48.0	-37 00 36	18.1	34134	35	E
524	01 05 49.4	-37 00 47	18.9	34098	38	E
524	01 05 41.7	-37 02 04	18.9	36382	29	E
524	01 05 46.4	-37 01 24	19.0	36241	56	E
524	01 05 50.2	-37 02 20	19.6	35954	29	E
524	01 05 52.7	-36 59 35	18.6	36487	35	E
526	01 06 30.5	-40 37 54	19.2	42036	50	E
526	01 06 37.9	-40 37 27	18.1	40912	47	E
526	01 06 24.0	-40 35 53	19.0	41095	32	E
526	01 06 29.4	-40 36 16	19.3	42522	56	E
526	01 06 21.5	-40 36 14	18.0	43215	32	E,AC
526	01 06 21.5	-40 35 10	18.8	43574	32	E
553	01 23 27.7	-39 44 15	16.7	26399	23	A
553	01 24 17.8	-39 45 09	18.5	26054	26	A
553	01 23 40.3	-39 44 49	17.9	26051	35	A
553	01 24 36.8	-39 50 08	18.6	26456	74	A
553	01 23 47.2	-39 47 38	17.5	26843	26	A
553	01 23 48.5	-39 48 58	18.2	26459	38	A
553	01 23 30.3	-39 45 20	17.5	26366	29	A
553	01 23 21.9	-39 44 43	18.5	26576	26	A
553	01 23 20.6	-39 52 25	17.4	26567	47	A
553	01 23 07.6	-39 45 20	17.7	24193	23	A,AC
553	01 23 16.7	-39 45 31	17.9	26702	65	A
553	01 23 14.2	-39 44 14	18.1	26645	80	A
553	01 23 10.4	-39 44 22	17.9	26273	17	A
553	01 23 43.5	-39 53 17	18.5	10504	26	A

EDCC	RA	DEC	$b_j$	cz	$\Delta cz$	Notes
555	01 23 48.2	-29 49 51	18.3	42531	59	E
555	01 23 46.8	-29 50 07	18.5	42474	68	E
555	01 23 45.6	-29 50 23	18.4	42543	80	E
555	01 23 10.2	-29 48 36	18.5	29040	41	E
557	01 23 44.5	-38 13 30	19.5	24067	299	E
557	01 23 49.3	-38 11 58	18.8	23395	44	E
557	01 23 50.8	-38 13 30	15.1	24094	35	E,AC
557	01 23 55.2	-38 12 17	17.4	24307	38	E
557	01 23 56.7	-38 14 40	18.1	23614	38	E
557	01 23 59.7	-38 12 05	19.4	23872	29	E
557	01 23 47.9	-38 13 03	18.9	25839	59	E
557	01 23 51.0	-38 13 30	15.1	23095	17	E,AC
570	01 30 14.9	-42 22 06	16.9	26249	29	E
570	01 29 47.3	-42 26 19	16.8	26250	23	E
570	01 29 49.2	-42 25 47	17.9	26519	32	E
570	01 30 15.4	-42 21 29	18.3	25074	44	E
571	01 30 03.4	-31 20 57	15.7	21336	47	E
571	01 30 11.6	-31 19 05	17.1	21815	62	E
571	01 30 12.7	-31 22 03	18.9	21719	83	E
571	01 30 05.9	-31 20 24	17.2	20808	38	E
571	01 30 07.2	-31 19 55	18.4	22847	98	E
575	01 31 36.8	-27 47 06	17.3	37021	35	E
575	01 31 34.8	-27 46 48	18.2	37854	29	E
575	01 31 33.1	-27 46 24	17.0	37357	35	E
575	01 31 45.0	-27 46 29	18.0	36910	41	E
575	01 31 38.3	-27 45 04	18.3	38904	29	E
575	01 31 30.4	-27 44 49	18.1	29049	140	E
575	01 31 48.1	-27 46 31	18.2	41086	41	E
591	01 41 52.0	-35 30 58	16.8	20895	26	E
591	01 41 55.0	-35 34 01	17.1	19810	68	E
591	01 41 57.9	-35 32 49	16.7	20442	32	E
591	01 41 54.3	-35 36 03	17.8	19612	26	E
591	01 42 06.2	-35 30 26	19.2	20598	80	E
591	01 41 57.2	-35 33 50	19.6	70993	137	E
591	01 42 03.0	-35 34 09	19.6	46176	41	E
591	01 42 05.2	-35 30 51	20.1	70568	164	E

EDCC	RA	DEC	$b_j$	cz	$\Delta cz$	Notes
606	01 58 20.5	-33 07 40	18.8	30815	41	E
606	01 58 20.3	-33 07 20	19.1	31819	32	E
606	01 58 20.4	-33 07 10	18.0	31217	38	E
606	01 58 20.2	-33 06 52	18.4	31235	35	E
606	01 58 53.9	-33 06 20	17.4	31493	47	E
606	01 58 51.2	-33 06 17	18.8	31328	68	E
606	01 58 29.4	-33 13 36	18.7	28510	23	E
606	01 58 33.4	-33 15 05	18.0	29130	59	E
606	01 58 33.7	-33 14 05	17.6	29028	26	E
606	01 58 35.2	-33 14 32	17.4	28899	29	E
606	01 58 38.5	-33 14 07	18.7	29136	32	E
606	01 58 49.1	-33 06 18	19.5	18449	38	E,AC
618	02 01 27.1	-41 21 25	19.0	37096	56	E,AC
618	02 01 30.4	-41 19 54	19.0	36157	50	E
618	02 01 31.4	-41 20 25	16.9	38100	47	E
618	02 01 34.8	-41 22 17	18.6	38412	35	E
618	02 01 37.6	-41 21 00	20.0	37336	35	E,AC
618	02 01 38.6	-41 21 41	20.3	37378	65	E
618	02 01 28.9	-41 22 11	19.6	43574	68	E
618	02 01 33.1	-41 20 07	18.0	35684	32	E
618	02 01 36.8	-41 20 50	18.9	40268	44	E
629	02 07 14.5	-37 33 39	16.3	27126	53	E
632	02 09 17.5	-40 31 17	19.9	30389	134	E
632	02 09 23.7	-40 31 42	18.9	31181	38	E
632	02 09 23.4	-40 32 04	18.6	30350	38	E
632	02 09 18.5	-40 29 50	20.0	31607	41	E
632	02 09 20.9	-40 31 11	18.0	29538	41	E
632	02 09 22.2	-40 32 07	19.0	29037	86	E
632	02 09 31.8	-40 32 16	19.7	71650	37	E
649	02 24 59.1	-26 40 39	17.4	44030	44	E
649	02 25 01.8	-26 40 06	18.3	44075	29	E
649	02 25 02.7	-26 40 13	19.3	44219	83	E
649	02 25 03.5	-26 41 34	18.7	43274	32	E
649	02 24 53.6	-26 42 00	17.8	17789	23	E
649	02 25 03.4	-26 41 05	17.4	24855	53	E
649	02 25 06.1	-26 42 08	16.7	10222	44	E

EDCC	RA	DEC	$b_j$	cz	$\Delta$ cz	Notes
653	02 28 42.4	-33 19 31	16.4	23557	35	E
653	02 27 14.4	-33 45 10	15.2	23131	35	E,AC
653	02 27 11.7	-33 43 40	16.5	23356	29	E,AC
653	02 28 50.0	-33 20 42	18.4	23995	59	E
653	02 28 05.6	-33 33 23	17.6	24154	74	E
653	02 28 02.8	-33 32 32	18.1	24343	101	E
658	02 27 21.6	-33 28 05	15.2	9635	194	E
658	02 29 57.4	-33 11 41	18.4	24082	29	A
658	02 28 44.1	-33 18 03	18.0	22004	59	A
658	02 30 01.5	-33 19 06	18.1	21656	62	A
658	02 29 48.0	-33 19 24	17.5	21267	32	A
658	02 29 40.6	-33 19 50	18.1	23554	26	A
658	02 29 06.1	-33 24 37	18.4	22667	20	A
658	02 28 40.3	-33 24 13	18.5	22502	29	A
658	02 28 36.5	-33 26 26	17.9	23413	50	A
658	02 28 02.8	-33 32 32	18.1	23953	74	A
658	02 28 04.8	-33 26 25	17.4	24214	65	A
658	02 28 04.6	-33 13 50	18.2	11344	35	A
658	02 28 45.1	-33 17 13	18.7	31274	29	A
658	02 28 48.1	-33 24 57	17.9	33597	71	A
658	02 29 00.9	-33 21 24	18.0	34071	71	A
658	02 28 42.4	-33 19 31	16.4	23560	32	A
658	02 28 03.7	-33 24 50	17.9	23317	17	A
658	02 27 48.8	-33 23 57	16.3	23827	44	A
658	02 28 35.7	-33 16 43	18.2	23317	26	A
658	02 28 08.9	-33 12 31	17.4	23233	26	A
658	02 28 43.8	-33 15 50	18.2	22325	17	A
658	02 28 29.3	-33 11 27	18.5	22994	17	A
658	02 28 18.2	-33 04 28	18.6	21638	29	A
658	02 28 28.0	-33 04 00	17.5	21779	38	A
658	02 28 48.9	-33 05 57	17.3	21923	71	A
658	02 29 12.0	-33 11 29	18.1	21309	23	A
683	02 42 57.9	-26 37 39	18.5	40304	50	E
683	02 43 00.8	-26 36 58	18.2	39875	83	E
683	02 42 09.7	-26 26 50	18.2	40016	35	E
683	02 42 08.8	-26 25 59	18.3	41290	47	E

EDCC	RA	DEC	$b_j$	cz	$\Delta$ cz	Notes
693	02 45 49.3	-42 03 59	17.8	21165	53	E
693	02 45 45.7	-42 03 35	16.9	21357	65	E
693	02 45 38.3	-42 02 40	17.4	41916	59	E
699	02 49 02.7	-25 08 07	19.8	33168	80	E
699	02 49 09.5	-25 07 36	18.3	33112	53	E
699	02 49 22.1	-25 15 02	17.8	33729	29	E
699	02 49 14.5	-25 09 36	18.9	33252	41	E
699	02 49 05.1	-25 07 50	19.3	10321	56	E
699	02 49 08.0	-25 08 06	19.1	35435	83	E
699	02 49 16.5	-25 10 37	19.6	34886	38	E
710	02 53 44.6	-22 52 00	17.7	37471	38	E
710	02 53 45.4	-22 50 46	18.8	37539	62	E
710	02 53 38.4	-22 54 00	19.0	37878	74	E,AC
710	02 53 41.7	-22 52 48	18.8	36694	50	E
712	02 54 25.5	-24 54 36	16.3	33133	29	A
712	02 54 51.1	-24 47 20	19.6	33396	53	A
712	02 54 36.4	-24 52 48	17.5	32038	32	A
712	02 54 42.7	-24 56 11	18.3	33396	50	A
712	02 54 34.7	-24 55 10	19.3	33555	59	A
712	02 54 31.8	-24 56 07	19.3	33399	32	A
712	02 54 21.3	-24 58 23	18.3	32896	41	A
712	02 54 20.9	-24 54 31	18.2	33324	146	A,AC
712	02 54 13.3	-24 58 46	17.9	33876	80	A
712	02 54 18.4	-24 53 45	19.2	34395	35	A
712	02 54 12.4	-24 55 30	19.8	32518	95	A
712	02 54 19.7	-24 52 57	19.5	33133	41	A
712	02 53 47.0	-24 51 55	19.0	33270	50	A
712	02 54 26.6	-24 49 19	18.9	47891	59	A
712	02 54 39.1	-24 45 15	17.7	28798	44	A
712	02 54 43.1	-24 52 06	19.8	37755	56	A
712	02 54 53.8	-24 45 05	18.1	25815	32	A
712	02 54 54.1	-24 56 55	17.4	38472	50	A
712	02 55 01.6	-24 51 46	18.9	40340	38	A
717	02 58 23.6	-37 07 07	14.9	19681	41	E
717	02 58 30.3	-37 14 51	15.6	20131	47	E
717	02 58 24.4	-37 14 20	16.7	19687	62	E

EDCC	RA	DEC	$b_j$	cz	$\Delta$ cz	Notes
722	03 00 44.6	-37 04 42	18.6	20137	38	E
722	03 00 48.4	-37 04 35	16.8	19819	32	E
722	03 00 39.6	-37 06 47	17.6	19846	38	E
722	03 00 32.2	-37 05 37	18.4	20116	44	E
726	03 04 45.8	-38 56 38	17.5	26339	35	E
726	03 04 40.1	-38 55 38	18.7	26066	50	E
726	03 05 01.5	-39 03 32	19.1	26201	50	E
726	03 04 59.5	-39 02 53	18.7	26165	20	E
728	03 06 40.6	-36 56 12	16.2	19768	44	A
728	03 05 59.0	-36 54 33	17.0	20131	38	A
728	03 05 33.7	-36 58 35	17.2	19783	89	A
728	03 05 36.4	-36 53 46	17.2	19972	35	A
728	03 04 41.6	-36 49 55	17.2	19918	38	A
728	03 06 32.8	-36 37 29	17.3	20526	98	A
728	03 06 17.7	-36 46 31	18.3	20427	56	A
728	03 06 24.0	-36 47 11	16.6	20673	65	A
728	03 05 13.6	-36 36 25	16.2	13286	59	A
735	03 09 25.9	-27 05 06	16.0	20526	44	E
735	03 09 09.8	-27 05 13	19.3	20958	98	E
735	03 09 13.6	-27 06 07	18.0	20403	17	E
735	03 09 16.4	-27 07 10	16.0	20475	41	E
735	03 09 13.4	-27 04 29	18.7	20403	47	E
735	03 09 20.6	-27 06 25	18.9	20763	23	E
735	03 09 16.4	-27 02 45	18.2	19717	41	E
735	03 09 15.1	-27 04 57	17.6	34718	65	E
735	03 09 19.4	-27 04 14	18.5	40429	77	E
742	03 11 49.0	-38 29 11	15.2	25611	53	E
742	03 11 38.0	-38 32 52	17.5	25443	68	E,AC
742	03 11 42.6	-38 31 21	18.5	25623	47	E
742	03 11 51.0	-38 28 39	18.9	25830	47	E
742	03 11 47.8	-38 29 44	18.1	24064	101	E
742	03 11 41.1	-38 32 54	17.2	24244	53	E
748	03 13 37.0	-29 31 25	17.2	19897	71	E
748	03 13 30.3	-29 30 37	16.7	19954	38	E
748	03 13 00.8	-29 20 29	17.1	19891	35	E

EDCC	RA	DEC	$b_j$	cz	$\Delta$ cz	Notes
748	03 12 53.4	-29 21 10	17.7	20541	56	E
748	03 12 54.0	-29 25 05	17.0	20176	47	E,AC
748	03 13 00.4	-29 25 18	17.1	20208	53	E
758	03 20 31.9	-41 32 25	15.7	19105	56	E
758	03 20 30.6	-41 31 31	18.3	19387	62	E
758	03 20 35.5	-41 31 41	18.2	18677	29	E
758	03 20 16.1	-41 30 16	17.9	19144	56	E
758	03 20 25.5	-41 33 39	20.2	19474	53	E
758	03 20 27.5	-41 34 03	19.3	18662	62	E
758	03 20 28.5	-41 31 11	15.5	19900	65	E
758	03 20 18.2	-41 30 30	17.0	20673	29	E
758	03 20 30.5	-41 34 09	19.7	20050	29	E
762	03 32 13.0	-39 10 37	15.8	18680	29	E
762	03 32 16.5	-39 09 33	16.0	18221	32	E
762	03 32 20.9	-39 11 48	16.4	19009	35	E
762	03 32 20.5	-39 09 21	17.9	20066	59	E
765	03 34 55.6	-39 57 55	16.0	31247	38	E
765	03 35 20.0	-39 58 50	18.6	31439	95	E
765	03 35 20.0	-39 58 50	18.6	31834	56	E
765	03 35 20.4	-39 58 30	17.2	31595	41	E
765	03 34 47.6	-39 57 25	16.0	19954	35	E,AC
765	03 35 18.1	-39 57 30	17.7	30255	38	E

Table 3: The galaxies observed in the EM cluster redshift survey at ESO and AAT. The columns represent: (1) The EDCC cluster identification name. (2) & (3) The equatorial coordinates (equinox 1950) from the EDSGC, RA and Dec respectively. (4) The approximate ( $\pm 0.25$  mag) apparent magnitude of the galaxy in the photographic  $b_j$  band from the EDSGC. (5) The heliocentric velocity of each galaxy in units of  $\text{km s}^{-1}$ . (6) The internal redshift error in units of  $\text{km s}^{-1}$  from the cross-correlation routine, described in section 4.2. (7) An “E” in this column denotes an ESO observation, “A” denotes an AAT observation, and an “AC” denotes a larger than normal error in the coordinates and magnitude. This is the case for galaxies which are not detected in the EDSGC, like e.g. objects merged with other object images in the digitization process. 2 galaxies in E178, 3 in E261, 2 in E424 and 3 in E473 do not have a certain identification in our logfiles (indicated as “NC”). We prefer therefore not to list any coordinate and magnitude which would be too approximate, although we give the redshift and the information that the object belongs to that cluster.

Table 4

EDCC	RA	DEC	N <sub>tot</sub>	N <sub>clus</sub>	cz	Δ cz	σ <sub>v</sub>	Notes
5	21 29 33.9	-22 53 02	6	3	33363	338	-	
42	21 46 21.9	-30 56 38	8	4	35294	103	-	
51	21 49 22.2	-29 08 02	6	5	27689	163	-	
57	21 53 30.9	-30 23 00	4	4	27754	97	-	
80	21 59 25.2	-22 48 38	36	29	21022	153	768(+128,-86)	
99	22 06 35.0	-27 33 24	4	-	-	-	-	p
114	22 11 08.7	-36 54 40	2	2	10183	-	-	
115	22 11 09.1	-35 13 31	4	3	21884	56	-	
124	22 14 43.9	-35 57 33	10	9	44188	388	1011(+397,-183)	
127	22 15 41.0	-39 08 56	14	-	-	-	-	p
131	22 16 39.2	-34 56 27	4	4	46884	266	-	
145	22 24 56.7	-30 51 11	12	11	17050	353	1105(+367,-184)	
172	22 35 50.4	-37 09 50	4	3	17542	284	-	
175	22 36 27.4	-38 05 29	4	3	46031	180	-	
178	22 37 50.6	-34 14 33	2	2	14905	56	-	
198	22 46 29.7	-41 10 02	6	-	-	-	-	p
201	22 47 13.5	-31 26 26	4	-	-	-	-	p
216	22 50 40.5	-25 47 14	5	-	-	-	-	p
230	22 56 32.8	-31 07 12	4	2	32916	611	-	
235	22 59 55.3	-33 38 06	4	-	-	-	-	p
247	23 02 56.1	-39 22 15	4	3	50116	335	-	
256	23 07 36.2	-23 12 40	4	-	-	-	-	p
261	23 09 09.0	-29 19 41	8	6	35614	375	820(+477,-173)	
269	23 12 32.5	-38 02 09	12	-	-	-	-	p
285	23 18 12.7	-42 09 25	4	-	-	-	-	p
297	23 23 46.2	-24 14 59	5	3	26752	186	-	
307	23 27 31.1	-39 33 25	3	3	16368	309	-	
311	23 28 36.0	-36 47 41	7	5	28829	217	-	
316	23 29 49.8	-36 31 28	4	4	28359	163	-	
326	23 35 09.7	-38 29 19	7	3	32592	110	-	
332	23 39 04.3	-29 28 46	3	3	15517	150	-	
348	23 44 33.7	-28 31 41	33	32	8757	151	830(+132,-90)	
366	23 52 19.6	-27 56 40	8	6	22040	204	464(+271,-100)	
372	23 54 18.2	-34 54 40	1	1	12675	-	-	
392	00 00 13.9	-34 56 38	8	7	33536	221	525(+261,-105)	
394	00 00 32.1	-36 12 59	6	6	14719	257	598(+348,-127)	
400	00 03 39.1	-34 58 49	10	7	34436	516	1222(+606,-243)	
408	00 07 27.8	-35 56 08	14	13	35864	272	871(+252,-136)	

EDCC	RA	DEC	N <sub>tot</sub>	N <sub>clus</sub>	cz	Δ cz	σ <sub>v</sub>	Notes
410	00 08 46.0	-29 07 35	2	2	18444	-	-	
418	00 12 30.2	-24 09 59	9	8	19714	267	706(+309,-134)	
419	00 12 49.7	-26 21 10	5	3	37215	955	-	
421	00 13 35.9	-35 13 53	7	5	43825	601	-	
424	00 14 05.9	-34 07 59	2	2	22629	-	-	
429	00 15 23.2	-35 25 03	19	17	29060	211	790(+188,-110)	
437	00 18 01.2	-25 54 26	6	5	18997	426	-	
438	00 20 23.5	-38 24 13	4	4	35797	401	-	
447	00 26 07.8	-23 54 04	6	4	33849	275	-	
448	00 26 34.0	-30 26 27	17	-	-	-	-	p
450	00 27 23.4	-29 45 01	5	4	29635	482	-	
460	00 34 47.1	-28 44 47	31	21	33610	170	700(+145,-90)	
462	00 35 14.5	-39 23 42	12	11	18864	183	569(+186,-95)	
470	00 37 26.4	-26 26 25	10	7	32903	175	415(+206,-83)	
471	00 37 43.3	-24 56 48	7	4	33519	262	-	
473	00 40 03.7	-28 50 23	14	13	32577	214	695(+200,-108)	
474	00 40 44.7	-26 19 54	15	8	33745	141	354(+156,-69)	
482	00 46 50.3	-29 47 22	30	21	32412	159	675(+138,-86)	
485	00 48 56.3	-28 46 50	6	6	33731	202	443(+258,-94)	
494	00 53 24.9	-37 36 36	4	4	16736	138	-	
495	00 53 28.6	-26 36 09	17	14	34213	121	403(+110,-61)	
499	00 53 51.4	-38 10 02	4	4	34877	203	-	
500	00 53 59.7	-30 20 02	7	3	33937	62	-	
519	01 02 07.7	-40 06 22	13	9	32100	138	371(+147,-69)	
520	01 02 11.5	-24 15 37	11	8	48025	370	902(+394,-170)	
524	01 05 39.9	-37 01 21	9	9	35232	364	975(+383,-176)	
526	01 06 30.7	-40 37 20	6	6	42224	443	950(+552,-199)	
553	01 23 09.0	-39 41 37	14	12	26449	70	242(+67,-39)	
555	01 23 24.9	-29 48 28	4	3	42518	22	-	
557	01 23 46.9	-38 14 35	8	6	23729	183	413(+240,-87)	
570	01 30 07.7	-42 24 39	4	4	26024	323	-	
571	01 30 15.4	-31 20 04	5	4	21421	230	-	
575	01 31 52.4	-27 47 19	7	5	37610	362	-	
591	01 41 46.0	-35 32 50	8	5	20272	242	-	
606	01 58 27.2	-33 11 15	12	11	30237	383	1152(+377,-190)	
618	02 01 28.8	-41 20 45	9	7	37166	368	865(+429,-172)	
629	02 07 12.0	-37 36 41	1	1	27126	-	-	
632	02 09 33.9	-40 31 42	7	6	30351	393	872(+507,-184)	



EDCC	RA	DEC	$N_{\text{tot}}$	$N_{\text{clus}}$	$cz$	$\Delta cz$	$\sigma_v$	Notes
649	02 24 54.3	-26 43 07	7	4	43900	212	-	
653	02 27 16.9	-33 41 37	6	6	23756	195	440(+257,-94)	
658	02 28 34.9	-33 17 56	26	22	22893	224	977(+194,-122)	
683	02 42 26.6	-26 31 11	4	4	40373	319	-	
693	02 45 51.1	-42 03 38	3	2	21261	-	-	
699	02 49 17.9	-25 09 01	7	6	33931	404	891(+518,-188)	
710	02 53 42.0	-22 51 30	4	4	37397	250	-	
712	02 54 19.6	-24 55 51	19	13	33256	161	519(+152,-81)	
717	02 58 55.5	-37 14 57	3	3	19834	149	-	
722	03 01 03.9	-37 07 47	4	4	19980	85	-	
726	03 04 43.0	-39 01 47	4	4	26194	56	-	
728	03 06 13.3	-36 53 32	9	8	20151	124	323(+142,-64)	
735	03 09 23.7	-27 05 34	9	7	20464	146	359(+179,-73)	
742	03 11 52.2	-38 30 35	6	6	25137	315	709(+413,-151)	
748	03 13 09.5	-29 24 14	6	5	20026	69	-	
758	03 20 22.1	-41 30 47	9	9	19453	220	618(+243,-112)	
762	03 32 15.2	-39 08 09	4	4	18994	392	-	
765	03 34 50.6	-39 53 16	6	4	31530	124	-	

Table 4: The clusters observed in the EM redshift survey. The columns represent: (1) The EDCC cluster identification name. (2) & (3) The equatorial RA and Dec coordinates (equinox 1950) of the cluster centroid, taken from Lumsden *et al.* 1992. (4) The total number of redshifts taken for each cluster (listed in Table 3). (5) The number of cluster members determined from the de-projection algorithm described in section 5.1. (6) The mean heliocentric redshift of the galaxy members in each clusters in units of  $\text{kms}^{-1}$ . (7) The  $1\sigma$  errors on the mean redshift of each cluster in units of  $\text{kms}^{-1}$ . (8) The radial velocity dispersions for clusters with  $N_{\text{clus}} \geq 6$  in units of  $\text{kms}^{-1}$ , along with the  $1\sigma$  errors (see section 6.1). (9) A “p” in this column indicates that the cluster has been classified as a projection effect (see section 5.2).

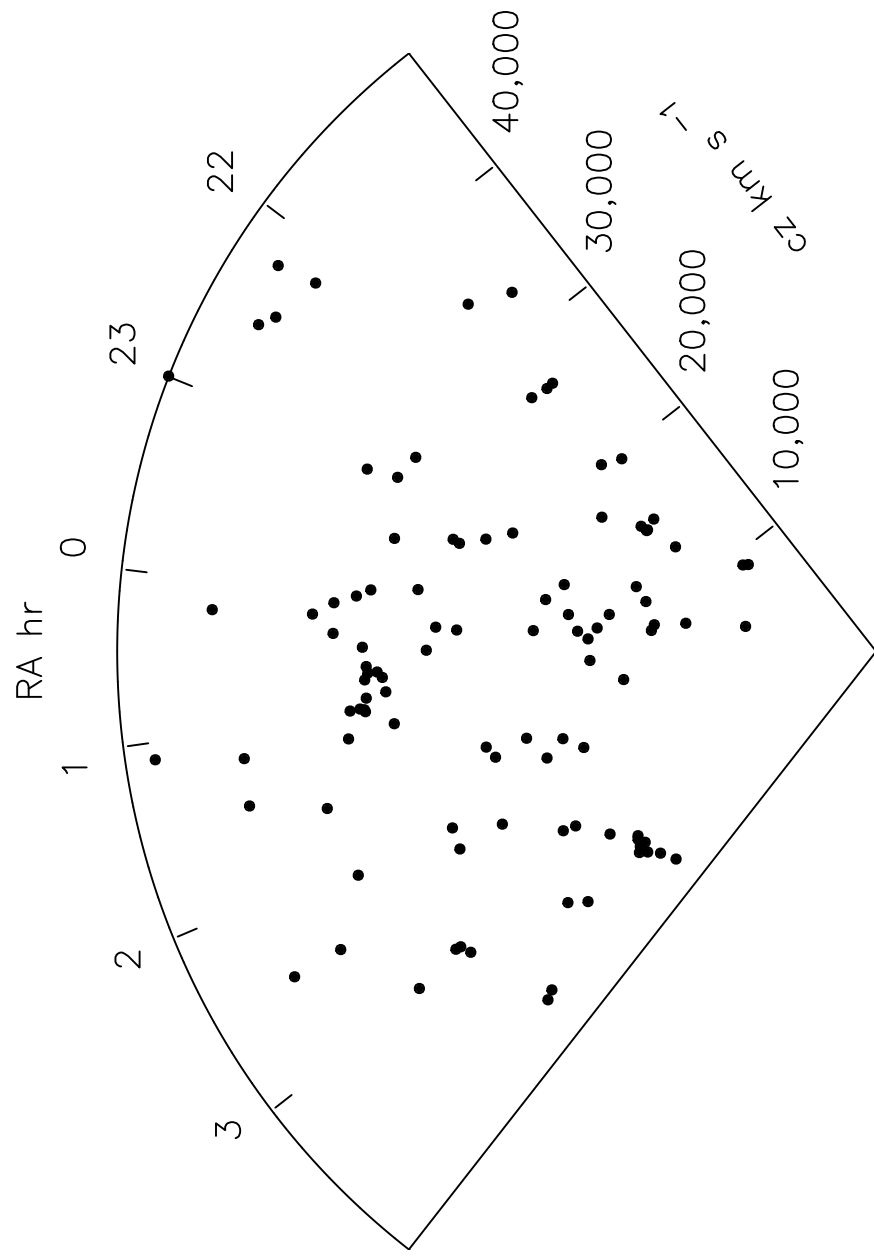
Table 5

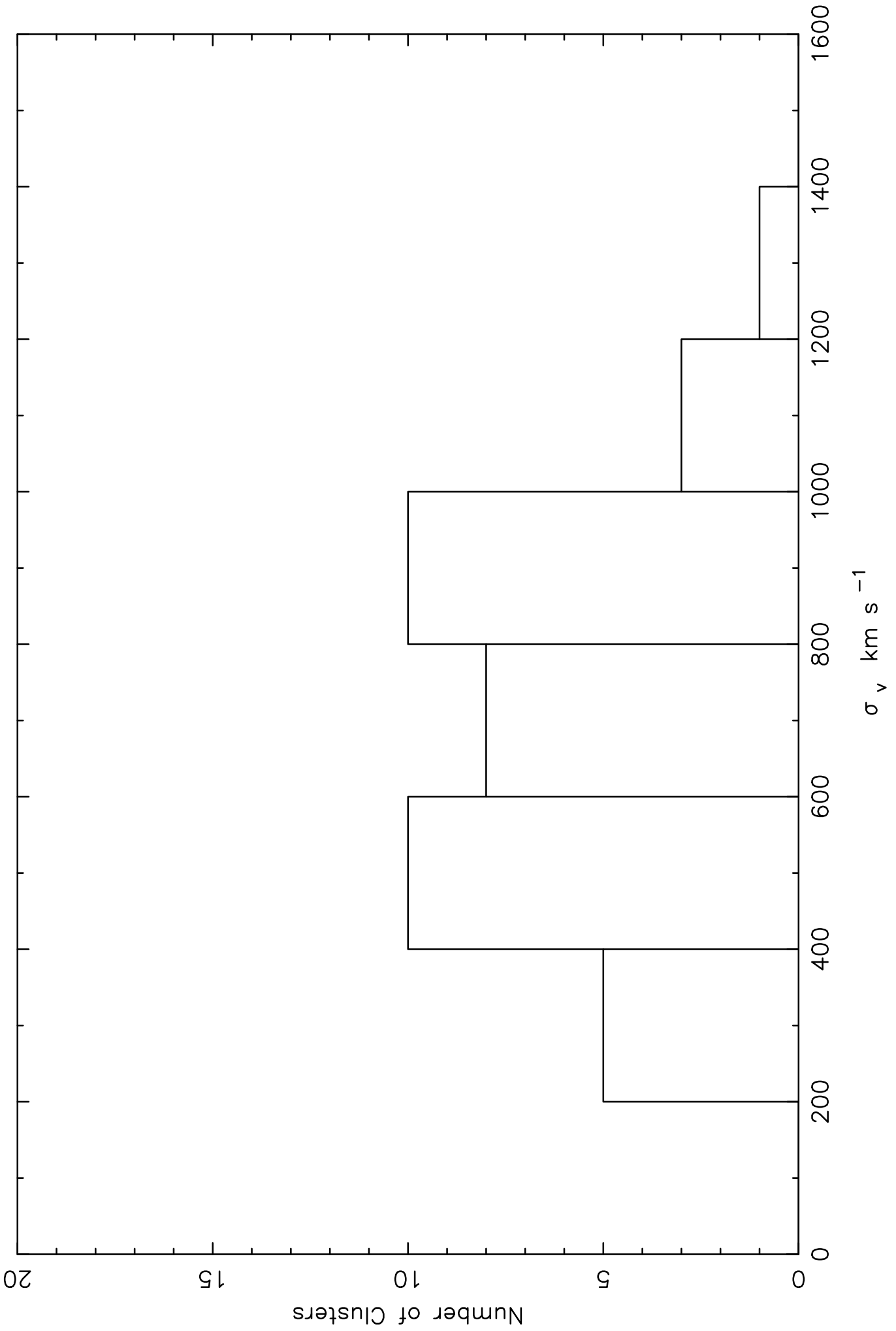
EDCC	RA	DEC	$R_1$	$m_{10}$	$\theta_A$	PA	$\epsilon$	$cz$	N	Reference
57	21 53 30.9	-30 23 00	59	18.1	0.172	32	0.24	27754	4	EM
72	21 56 56.9	-42 20 24	30	18.3	0.157	83	0.57	-	-	-
80	21 59 25.2	-22 48 39	26	17.7	0.202	-	-	21022	29	EM
86	22 02 26.5	-30 45 48	26	18.7	0.136	138	0.45	28180	1	Loveday (1991)
114	22 11 08.7	-36 54 40	24	17.2	0.245	65	0.57	10183	2	EM
124	22 14 43.9	-35 57 33	75	18.7	0.127	115	0.60	44188	9	EM
127	22 15 41.0	-39 08 56	67	18.5	0.145	-	-	-	-	EM (projection)
129	22 16 02.1	-24 26 56	28	16.8	0.30	97	0.18	10463	2	Loveday (1991)
145	22 24 56.7	-30 51 11	35	17.	0.271	132	0.21	17050	11	EM
160	22 31 32.4	-37 59 54	77	18.7	0.138	11	0.22	45269	70	Teague <i>et al.</i> (1990)
165	22 33 35.6	-24 36 25	25	17.7	0.197	116	0.40	-	-	-
172	22 35 50.4	-37 09 50	25	17.3	0.357	89	0.73	17542	3	EM
173	22 35 57.3	-36 39 56	31	18.0	0.265	77	0.74	17058	-	Peacock (priv. comm.)
175	22 36 27.4	-38 05 29	34	18.5	0.148	179	0.77	46031	3	EM
176	22 36 54.3	-36 26 25	35	18.3	0.237	-	-	17088	1	Nicholson (1991)
178	22 37 50.6	-34 14 33	28	18.2	0.161	24	0.61	14905	2	EM
188	22 43 39.4	-36 21 47	35	17.5	0.219	139	0.49	20116	3	Muriel <i>et al.</i> 1990
201	22 47 13.5	-31 26 26	37	18.4	0.155	-	-	-	-	EM (projection)
203	22 48 13.2	-26 20 35	34	18.3	0.153	168	0.51	-	-	-
216	22 50 40.5	-25 47 14	58	18.2	0.163	-	-	-	-	EM (projection)
230	22 56 32.8	-31 07 12	33	18.6	0.141	-	-	32916	2	EM
258	23 08 01.3	-22 55 15	35	18.7	0.131	41	0.39	33547	1	Ciardullo <i>et al.</i> 1985
260	23 08 28.2	-28 59 43	30	18.7	0.131	103	0.66	-	-	-
261	23 09 09.4	-29 19 41	22	18.4	0.152	147	0.37	35614	6	EM
263	23 09 23.8	-41 02 21	29	18.7	0.133	86	0.31	-	-	-
269	23 12 32.5	-38 02 09	44	18.6	0.140	-	-	-	-	EM (projection)
279	23 15 47.7	-27 47 17	22	18.6	0.138	177	0.45	25182	1	Nicholson (1991)
285	23 18 12.7	-42 09 25	30	17.7	0.199	-	-	-	-	EM(projection)
297	23 23 46.2	-24 14 59	42	18.3	0.159	68	0.76	26752	3	EM
311	23 28 36.0	-36 47 41	43	18.1	0.253	-	-	28829	5	EM
316	23 29 49.8	-36 31 28	49	17.4	0.343	43	0.59	28359	4	EM
332	23 39 04.3	-29 28 46	34	17.8	0.194	54	0.30	15517	3	EM
335	23 39 36.3	-30 28 45	23	18.7	0.136	102	0.61	21015	1	Olowin <i>et al.</i> (1988)
348	23 44 33.7	-28 31 41	22	16.2	0.430	130	0.44	8757	32	EM
366	23 52 19.6	-27 56 40	33	17.7	0.205	153	0.32	22040	6	EM
377	23 56 26.4	-32 09 32	53	17.8	0.185	29	0.41	17748	1	Broadbent 1992 (priv. comm.)
381	23 57 14.2	-39 45 34	22	18.5	0.145	11	0.52	30455	1	Muriel <i>et al.</i> (1991)
387	23 58 35.2	-36 39 00	27	18.6	0.134	73	0.28	-	-	-
392	00 00 13.9	-34 56 38	34	18.6	0.140	128	0.28	33536	7	EM
394	00 00 32.1	-36 12 59	24	17.4	0.227	148	0.21	14719	6	EM

EDCC	RA	DEC	$R_1$	$m_{10}$	$\theta_A$	PA	$\epsilon$	$cz$	N	Reference
396	00 00 37.9	-27 28 16	22	18.3	0.159	116	0.61	20416	3	Postman <i>et al.</i> (1992)
398	00 01 25.3	-23 25 16	29	18.6	0.140	98	0.33	-	-	-
400	00 03 39.1	-34 58 49	80	18.5	0.147	170	0.21	34436	7	EM
407	00 06 38.9	-35 35 00	25	17.7	0.196	144	0.21	14870	3	Huchra <i>et al.</i> (1992)
410	00 08 46.0	-29 07 35	25	17.4	0.225	172	0.23	18444	2	EM
418	00 12 30.2	-24 09 59	32	17.1	0.264	35	0.22	19714	8	EM
419	00 12 49.7	-26 21 10	35	18.7	0.133	74	0.70	37215	3	EM
424	00 14 05.9	-34 07 59	22	18.4	0.141	11	0.23	22629	2	EM
429	00 15 23.2	-35 25 03	63	18.0	0.176	4	0.56	29060	17	EM
431	00 16 17.4	-42 01 24	30	18.2	0.166	79	0.73	27671	3	Muriel <i>et al.</i> (1991)
437	00 18 01.2	-25 54 26	59	18.5	0.145	95	0.57	18998	5	EM
446	00 25 44.0	-35 43 05	22	18.7	0.130	125	0.81	-	-	-
447	00 26 07.8	-23 54 04	46	18.4	0.152	3	0.49	33849	4	EM
448	00 26 34.0	-30 26 27	22	18.7	0.181	-	-	-	-	EM (projection)
450	00 27 23.4	-29 45 01	26	18.5	0.143	54	0.38	29635	4	EM
460	00 34 47.1	-28 44 47	30	17.9	0.183	62	0.10	33610	21	EM
462	00 35 14.5	-39 23 42	35	18.5	0.147	49	0.62	18864	11	EM
473	00 40 03.7	-28 50 23	44	18.0	0.265	112	0.62	32577	13	EM
474	00 40 44.7	-26 19 54	22	18.6	0.203	7	0.43	33745	8	EM
480	00 45 56.6	-42 17 21	23	18.5	0.141	40	0.20	-	1	Huchra (priv. comm.)
482	00 46 50.3	-29 47 22	54	18.0	0.177	139	0.24	32412	21	EM
495	00 53 28.6	-26 36 09	55	18.1	0.176	62	0.16	34213	14	EM
500	00 53 59.7	-30 20 02	40	18.8	0.134	37	0.62	33937	3	EM
505	00 54 38.9	-29 57 01	26	18.5	0.147	-	-	-	-	-
507	00 54 55.5	-26 33 36	23	18.4	0.155	143	0.26	33811	1	Peterson <i>et al.</i> (1986)
519	01 02 07.7	-40 06 22	37	18.2	0.164	8	0.43	32100	9	EM
520	01 02 11.5	-24 15 37	70	18.6	0.138	125	0.19	48025	8	EM
524	01 05 39.9	-37 01 21	55	18.6	0.137	153	0.34	35232	9	EM
546	01 19 45.7	-39 53 30	27	18.6	0.141	157	0.54	-	-	-
553	01 23 09.0	-39 41 37	25	18.1	0.168	146	0.53	26449	12	EM
555	01 23 24.9	-29 48 28	22	18.4	0.148	161	0.59	42518	3	EM
557	01 23 46.9	-38 14 35	42	18.1	0.168	39	0.29	23729	6	EM
570	01 30 07.7	-42 24 39	29	17.9	0.185	31	0.46	26024	4	EM
575	01 31 52.4	-27 47 19	29	18.0	0.175	44	0.27	37610	5	EM
587	01 39 46.9	-42 24 58	31	17.6	0.214	18	0.42	22790	-	Dalton <i>et al.</i> 1994
591	01 41 46.0	-35 32 50	28	17.6	0.211	2	0.22	20272	5	EM
606	01 58 27.2	-33 11 15	33	18.	0.179	62	0.43	30237	11	EM
618	02 01 28.8	-41 20 45	30	18.4	0.153	122	0.41	37166	7	EM
645	02 23 11.7	-29 43 25	30	18.1	0.170	161	0.56	-	-	-
653	02 27 16.9	-33 41 37	30	18.3	0.153	67	0.33	23756	6	EM

EDCC	RA	DEC	$R_1$	$m_{10}$	$\theta_A$	PA	$\epsilon$	cz	N	Reference
658	02 28 34.9	-33 17 56	43	18.5	0.141	79	0.48	22893	22	EM
683	02 42 26.6	-26 31 11	22	18.3	0.162	136	0.59	40373	4	EM
699	02 49 17.9	-25 09 01	65	18.2	0.163	119	0.10	33931	6	EM
700	02 49 39.5	-25 47 16	27	18.4	0.151	121	0.56	33577		Peacock (priv. comm.)
707	02 51 30.2	-33 41 40	26	17.9	0.187	8	0.62	-	-	
712	02 54 19.6	-24 55 51	26	18.6	0.138	19	0.53	33256	13	EM
717	02 58 55.5	-37 14 57	43	17.3	0.241	144	0.63	19834	3	EM
726	03 04 43.0	-39 01 47	26	18.5	0.143	158	0.44	26194	4	EM
728	03 06 13.3	-36 53 32	38	17.3	0.237	34	0.16	20151	8	EM
729	03 06 15.5	-23 53 09	24	17.4	0.225	107	0.13	19736	2	Postman <i>et al.</i> (1992)
735	03 09 23.7	-27 05 34	22	17.4	0.230	146	0.65	20464	7	EM
742	03 11 52.2	-38 30 35	25	17.9	0.187	172	0.39	25137	6	EM
748	03 13 09.5	-29 24 14	29	17.7	0.202	106	0.49	20026	5	EM
758	03 20 22.1	-41 30 47	36	17.9	0.187	41	0.13	19453	9	EM
762	03 32 15.2	-39 08 09	23	17.3	0.236	68	0.31	18994	4	EM
763	03 32 55.2	-39 38 01	25	18.2	0.152	88	0.63	30879		Peacock (priv. comm.)
765	03 34 50.6	-39 53 16	22	18.0	0.177	134	0.18	31530	4	EM

Table 5: The list of clusters selected from the EDSGC using a reduced Abell radius of  $1.0 h^{-1}$  Mpc and subject to the selection criteria given in section 7, used as the basis for the clustering analysis of Nichol *et al.* 1992 (see section 7) and Martin *et al.* 1994. The columns represent: (1)–(3) The EDCC identification and coordinates as given in Table 4. (4) The number of galaxy members between the magnitudes  $m_3$  and  $m_3 + 2$  calculated using an Abell radius of  $1 h^{-1}$  Mpc. (5) Magnitude of the  $10^{\text{th}}$  brightest galaxy, after background correction, within the  $1 h^{-1}$  Mpc radius. (6) The angular ‘reduced Abell radius’ calculated using the equivalent of Abell’s  $m_{10}$  distance estimate. (7) The position angle of the cluster, in degrees measured from the North clockwise, as defined in Martin *et al.* (1994). This parameter is not used in this paper but is included here for completeness. (8) The eccentricity of the clusters defined as the ratio between the minor and the major axis of the cluster, as defined and used in Martin *et al.* 1994. (9) The radial velocity of the cluster in units of  $\text{kms}^{-1}$ . (10) The number of galaxies used to determine cz. For the EM clusters, this is just  $N_{\text{clus}}$ . (10) The source of the cluster radial velocity.





# The EDSGC – VII: The Edinburgh–Milano Cluster Redshift Survey <sup>★</sup>

C.A. Collins<sup>1</sup>, L. Guzzo<sup>2</sup>, R.C. Nichol<sup>3</sup>, S.L. Lumsden<sup>4</sup>

<sup>1</sup>*Astrophysics Group, School of Chemical and Physical Sciences, Liverpool John Moores University, Byrom Street, Liverpool, L3 3AF U.K. – cac@star.livjm.ac.uk*

<sup>2</sup>*Osservatorio Astronomico di Brera, Via Bianchi 46, I-22055 Merate, Italy – guzzo@astmim.mi.astro.it*

<sup>3</sup>*Department of Astronomy and Astrophysics, University of Chicago, 5640 S. Ellis Rd., Chicago, IL 60637, USA – nichol@huron.uchicago.edu*

<sup>4</sup>*Anglo-Australian Observatory, Epping Laboratory, PO Box 296, Epping NSW 2121, Australia – sll@aaopp2.aao.gov.au*

Accepted December 1994

## ABSTRACT

In this paper we present the redshifts of the galaxies and galaxy clusters which form the Edinburgh–Milano (EM) cluster redshift survey. A total of 777 galaxy redshifts have been measured in 94 clusters extracted from the digitised Edinburgh Durham Cluster Catalogue. We also present the radial velocity dispersions for 37 clusters. Observational and data reduction techniques are discussed in detail, together with the strategy adopted to determine the mean redshift of a cluster and to identify and discard plausible phantom clusters. Some 10% of our clusters show heavy contamination, indicating that projection is a serious problem for optically selected rich clusters. The median velocity dispersion estimated for a sub-sample of richness  $R \geq 1$  clusters is  $742 \pm 63 \text{ km s}^{-1}$ . From a simple comparison with  $\Omega = 1$  Cold Dark Matter models of structure formation, these results favour a biasing parameter  $b = 1.6 - 2.0$  and are inconsistent with a bias outside of the range  $b = 1.3 - 2.5$ .

**Key words:** Redshift Surveys — Catalogues — Galaxy Clusters — Cosmology — Large-Scale Structure.

## 1 INTRODUCTION

Clusters of galaxies represent one of the most important probes of the universe on cosmologically interesting scales. With typical separations of  $\simeq 10 - 20 h^{-1} \text{ Mpc}$ , their spatial distribution can be used to map the underlying matter distribution on scales which can discriminate between the various models of structure formation (e.g. Mann, Peacock & Heavens 1994; Croft & Efstathiou 1994; Borgani *et al.* 1995). These models can also be constrained by examining the dynamical properties of clusters (e.g. Frenk *et al.* 1990). The Abell catalogue (Abell 1958) and its southern counterpart (Abell, Corwin & Olowin 1989) have been the most widely used source of rich galaxy clusters. As such, the primary cluster redshift surveys used to study large-scale structure in the universe have concentrated on Abell clusters. To date, the largest single compilation of Abell clusters is that of Struble & Rood (1991a), who list 758 redshifts and

121 velocity dispersions, although this compilation ignores southern ACO and supplementary clusters.

One of the major scientific investigations using such samples of Abell clusters has been the determination of the amplitude of the clustering pattern of rich clusters. Bahcall & Soneira (1983) studied the clustering of a statistical sample of 104 clusters which constitutes all the high galactic latitude  $R \geq 1$  and  $D \leq 4$  Abell clusters, by estimating the two-point cluster correlation function  $\xi_{cc}(r)$ . More recently, Postman, Huchra & Geller (1992) have estimated  $\xi_{cc}(r)$  for a complete sample of 351 Abell clusters with tenth ranked galaxy magnitudes ( $m_{10}$ )  $\leq 16.5$ . The results from these two studies are consistent in showing a correlation function of the form  $\xi_{cc}(r) = (r/r_0)^{-1.8}$ , with a correlation length  $r_0 \geq 20 h^{-1} \text{ Mpc}$ . In addition, Peacock & West (1992) have carried out a power-spectrum analysis of a volume limited all-sky cluster sample containing 427 Abell clusters, which is  $\sim 90\%$  complete in redshift for richness class  $R \geq 0$ . This study implies a similar correlation length.

However, these results have been challenged due to alleged systematic errors in the Abell catalogue, which could artificially enhance the value of  $r_0$  (Lucy 1983, Sutherland

<sup>★</sup> Based mainly on data collected at the European Southern Observatory, La Silla, Chile.

1988, Dekel *et al.* 1989, Efstathiou *et al.* 1992). These systematics could be due to selecting clusters visually from photographic plates, or patchy Galactic extinction, or contamination of galaxy associations — which are simply projected enhancements along the line-of-sight. A significant step towards a more objective understanding of the nature of the galaxy distribution has been realised with the construction of digitised galaxy catalogues, such as the Edinburgh/Durham Southern Galaxy Catalogue (EDSGC, Heydon-Dumbleton *et al.* 1989) and the APM catalogue (Maddox, Efstathiou & Sutherland 1990). From these surveys, it has been possible to select clusters automatically and produce cluster samples which are not prone to the subjective effects discussed above. Specifically, from the EDSGC we have constructed the Edinburgh/Durham Cluster Catalogue (EDCC), consisting of 737 clusters over an area of  $1500 \text{ deg}^2$ , centered at the South Galactic Cap (Lumsden *et al.* 1992). The EDCC is complete to  $b_j = 18.75$ , approximately 1 magnitude fainter than the Abell catalogue. A comparison with the Abell cluster catalogue in the same region of sky reveals that to the completeness limit of the EDCC, 80% of Abell clusters are detected. All aspects of the catalogue construction and a detailed listing of the clusters themselves are given in Lumsden *et al.* (1992).

During the last five years we have been measuring redshifts for galaxies in the EDCC. Our aim was to assemble a complete richness-limited spatial sample of clusters, with accurately known redshifts. To this end, a mean number of  $\sim 10$  galaxies per cluster was observed, a strategy that characterizes our survey and allowed a further check of residual projections. This survey is called the Edinburgh/Milano (EM) cluster redshift survey, and it is presented in detail in this paper. Previous papers related to the analysis of this data set have discussed the large-scale distribution (Guzzo *et al.* 1992), the correlation function of the clusters (Nichol *et al.* 1992), and large-scale cluster alignments (Martin *et al.* 1995). These analyses have indicated a lower level of clustering of rich clusters than implied by the Abell catalogue, with a correlation length  $r_0 \simeq 15 h^{-1} \text{ Mpc}$ . In addition to the data, we present here also an analysis of the velocity dispersion for a subset of 37 clusters.

The paper is organized as follows. In section 2 we describe in detail the observational procedures adopted at ESO and the AAT. In section 3 we discuss the reduction of the data to 1-D spectra and in section 4 we explain the galaxy redshift determinations. In section 5 we describe the determination of each cluster redshift, along with an explanation of how we identify clusters as projection effects. In section 6 we present the cluster velocity dispersions and briefly discuss their implications for cosmology. In section 7 the EDCC cluster sample used to determine the correlation function is defined, as the exact selection criteria used for the correlation function sample differs from the manner in which the EDCC was selected in certain important respects.

## 2 OBSERVATIONS

### 2.1 Observing Strategy

In adopting a strategy for taking the redshift of clusters, our main concern was the problem of galaxy interlopers and

phantom clusters caused by the alignment, along the line-of-sight, of small groups of galaxies. Lucey (1983) argues that the Abell catalogue contains a significant fraction of heavily contaminated clusters. His models indicate that between 15–25% of the clusters in the Abell catalogue have a true galaxy population that is less than half of their observed population. Although there are counter arguments suggesting that the contamination is not that significant (Struble & Rood 1991b), this point can only really be addressed by taking multiple redshift measurement towards the cores of the clusters. The majority of existing cluster redshift surveys are based mainly on one or two galaxy redshift measurements per cluster. For example,  $\sim 68\%$  of the cluster redshifts in the Struble & Rood (1991a) compilation are based on  $< 3$  galaxies and the two largest systematic cluster redshift surveys to date, the Abell-based survey of Postman *et al.* (1992) and the APM survey (Dalton *et al.* 1994), contain significant fractions of single or double cluster redshift measurements. The APM survey contains 188 clusters, of which  $\sim 70\%$  are based on 1 or 2 galaxy redshifts; while for the Postman sample, the figure is  $\sim 50\%$ . Phantom clusters cannot be detected with so few redshifts, while for real clusters, there is a finite chance that the redshift of an interloper will be measured and assigned to the cluster. Therefore, the strategy behind the construction of the EM redshift survey was to measure about 10 galaxy redshifts per cluster towards the centres of the rich clusters selected from the EDCC.

### 2.2 ESO Observations

Over 70% of all the observations made in the construction of the EM survey were carried out using the ESO Faint Object Spectrograph and Camera (EFOSC) on the 3.6 m telescope at La Silla, Chile. EFOSC is a high-efficiency transmission spectrograph, with multi-object spectroscopic capability (MOS) and fast switching to imaging mode. This latter feature allows very accurate slit positioning on faint objects. At the time of our observations (1988–1991), the detector was a thinned, back-illuminated RCA CCD chip of size  $520 \times 320$  pixels, with good response in the blue band. The pixel size with this setup is  $30 \mu\text{m}$ , corresponding to  $0.675 \text{ arcsec}$  on the sky and the dispersion direction runs along the longest CCD axis. The chip is cosmetically clean with a read-out noise of 45 electrons. The peak quantum efficiency of the chip is reached at  $4800 \text{ \AA}$  and remains  $> 60\%$  over the observed wavelength range.

EFOSC was mainly used in MOS mode, which entailed producing masks of the clusters which were then inserted into free positions in the aperture wheel of the spectrograph (see below). For single slit observations, we used a 2-arcsec wide slit, the same width obtainable on the MOS masks. We used the B300 grism which has a dispersion of  $230 \text{ \AA}/\text{mm}$ . With the RCA chip this corresponds to a resolution of  $6.9 \text{ \AA}$  per pixel, providing a wavelength coverage between  $3600 \text{ \AA} - 7000 \text{ \AA}$ . With this setup, spectral resolution as measured on a purely instrumentally broadened line resulted in about 2 pixels FWHM. Using a cross-correlation technique, this moderate resolution enabled us to achieve an *rms* external error on the radial velocities of  $\sim 140 \text{ km s}^{-1}$  (see section 4.2).

MOS operations with EFOSC involve the use of pre-

prepared masks on which slitlets of length 5 – 30 arcsec are punched. Their positions on the mask are determined from a direct CCD image of the cluster. On average each mask contained 10 – 15 slitlets, with a maximum of 22 for the cluster E429. The integrations were carried out in two consecutive exposures each of 20 – 30 minutes duration which facilitated the removal of cosmic-ray events. He–Ar calibration spectra were observed before and after the science exposures through the same mask. A few clusters, not suitable for MOS were observed in single-slit mode. Standard bias frames and flat-fields were taken at the beginning and end of each night.

A limited number of redshifts were obtained at the ESO 2.2 m telescope. For these observations a classical Boller & Chivens spectrograph coupled with an RCA CCD was used, with a spectral setup similar to that adopted for EFOSC. During these runs we also re-observed some of the clusters already secured with the 3.6 m, in an effort to establish external redshift errors (see section 4.2).

### 2.3 AAT OBSERVATIONS

About 30% of the survey data were collected during a 3-night run at the Anglo–Australian 3.9 m Telescope (AAT) using the multi-fibre spectrograph AUTOFIB coupled to the RGO spectrograph. This instrument has 60 user fibres that are automatically positioned by a flying robot over a circular field of 40 arcmin in diameter at the Cassegrain focus of the AAT. Full instrumental details are given in Parry & Sharples (1988). The optimum instrumental combination proved to be the 600V grating in conjunction with the IPCS. However, due to technical constraints, half the clusters were observed using the GEC CCD. Both detectors provide a wavelength coverage 3700 Å – 5500 Å, with a resolution of 3 Å per pixel for the CCD and 1.7 Å for the IPCS.

The positions of the target galaxies, to be fed into the system controlling AUTOFIB for positioning the 2 arcsec fibres, were taken from the EDSGC, which provides a positional accuracy of  $\simeq 1$  arcsec. The galaxy target list was constructed by giving priority to bright galaxies near the centre of the clusters. Within the mechanical constraints we observed 30 – 40 galaxies per cluster, with the remaining fibres placed on the sky near concentrations of object fibres. The sequence of object and calibration exposures was the same as that adopted for the ESO observations. Finally, for both the ESO and AAT observations, radial velocity standard stars were observed on most nights.

## 3 DATA REDUCTION

### 3.1 EFOSC Data

After subtracting the bias, the two science exposures available for every MOS observation were averaged together using a  $k$ -sigma clipping algorithm, which very effectively removed most of the cosmic ray events. The data were reduced using the MIDAS package. When necessary, appropriate programmes were developed to facilitate the reduction of the multi-object data (extraction of single spectra, wavelength calibration and sky subtraction). The lamp flat-fields were normalized by removing the large-scale spectral response

of the lamp before being used, leaving only the pixel-to-pixel variations. These proved to be very small ( $\simeq 2\%$ ) and had negligible effect on the estimate of line positions. For each MOS frame, the first arc spectrum was searched for a number of calibration lines, a few of which were manually identified. Supplemented by an automatic search, this typically resulted in  $\simeq 15$  lines which were used to calculate the pixel-to-wavelength relationship to be applied to the corresponding science spectrum. The typical *rms* wavelength calibration error using a 3rd order polynomial was  $\sim 0.3$  Å. The object spectrum was then rebinned into constant wavelength steps of 5 Å. A further test of the accuracy of the wavelength calibration was performed by checking the wavelength of sky emission lines from the calibrated spectrum against their nominal value.

Once the spectrum from the first slitlet was calibrated, the approximate zero-point shift of the following arc in the same MOS exposure was found by pointing to a bright Helium line. This was used by the program as a first guess to re-identify the calibration lines and find a new wavelength solution for the second spectrum. The process continued until all the spectra in the MOS frame were calibrated. The whole procedure could be checked in real time and, if necessary, paused to correct for misidentified lines. The resulting calibrated spectra were then reduced to one dimension and sky subtracted. Since some spectra did not have sky on the slit, performing this operation after wavelength calibration allowed us to use the sky from an adjacent slit when necessary. For most of the objects sky subtraction was very effective (a clear advantage of slitlets compared to fibres). All the resulting 1-D spectra were directly inspected and sky-line residuals removed by linear interpolation of the galaxy continuum across the line.

Over the six ESO observing runs, a total of  $\simeq 544$  galaxy spectra were observed. Fig. 1 shows some typical galaxy spectra selected from the ESO database.

### 3.2 AUTOFIB Data

It was decided not to flat-field either the CCD or IPCS data, as the pixel to pixel response of both detectors had negligible effect on the line positions. Fibre spectra were then extracted from the parent frames using dedicated commands within the FIGARO package. This automatically applied a correction for S distortion in the dispersion direction. The final product was a reduced 2-D data frame, within which each of the 55 – 60 rows corresponded to a different spectrum. The arcs taken for these data proved to contain only low signal-to-noise lines. In order to increase the signal to noise, we explored the possibility of co-adding all the calibration arcs taken on the same night. It was found that the *rms* temporal shifts in the arcs was  $\sim 0.05$  pixels, which is one order of magnitude lower than the expected *rms* calibration residuals. Given this negligible shift, we constructed a master arc for each night to calibrate all the spectra in each 2-D frame. The master arc provided 40 – 50 identified lines spread evenly throughout the wavelength window. The calibration relation was then obtained by a 4th order polynomial fit, which gave a typical *rms* residual of  $\sim 0.3$  Å for the IPCS data and  $\sim 0.7$  Å for the CCD data. As a final verification of the accuracy of the wavelength calibration, we



checked the stability of the  $[\text{O I}]\lambda 5577 \text{ \AA}$  sky line over the whole night. This was found to be at the correct wavelength with an *rms* deviation similar to that quoted above.

There is no generally agreed optimal procedure for sky-subtraction using fibres (see Ellis & Parry 1988). One possibility is to dedicate some fibres to the sky only and then re-normalize their relative transmission. This can be achieved by measuring ‘offset skies’ before or after the science exposure by offsetting the telescope by a small amount and taking a short sky exposure through the configured fibres. With this method the degree of bending and torsion in the fibres remains close to that in the science exposure thereby preserving the relative transmission. However, to obtain a sufficient signal-to-noise ratio, sky exposures  $\geq 15$  minutes duration are required and for this reason we did not adopt this strategy. Instead, we constructed a median sky spectrum from all the sky fibres, after dividing each single sky fibre spectrum by its median count. Then we used the ratio of the heights of the  $[\text{O I}]\lambda 5577 \text{ \AA}$  sky lines to scale the median sky to each fibre response and subtracted. This technique proved to be very successful (see Nichol 1992), and has been recently discussed in detail in other papers (e.g. Lissandrini, Cristiani & La Franca 1994; Ettori, Guzzo & Tarenghi 1995).

#### 4 GALAXY REDSHIFT DETERMINATION

To estimate the redshifts from the calibrated spectra we used the cross-correlation technique described in detail by Tonry & Davis (1979), in the version developed within FIGARO which closely follows the original prescription. The basis of the technique is the cross-correlation of the observed galaxy spectrum with a model or template spectrum. This is performed by taking the Fast Fourier Transform of the two spectra, multiplying them together and then transforming back the result to get the Cross-Correlation Function (CCF), whose highest peak is related to the radial velocity difference between the two spectra. Before actually starting this machinery, the two spectra are rebinned into logarithmic bins, so that the relative redshift becomes a linear shift between the two and a number of operations are performed on them to improve the quality of the final result. These are described in detail by Tonry & Davis (1979), and include continuum subtraction, cosine-bell apodizing and bandpass filtering. All these operations were performed using FIGARO specific commands, and several combinations of the parameters involved were tested to find the most appropriate set for our spectra. In particular, the spectra were rebinned into 2048 logarithmic bins. For the ESO data, this corresponded to a velocity binwidth of  $84.5 \text{ km s}^{-1}$ , while for the AUTOFIB data it was  $57.9 \text{ km s}^{-1}$ . The redshift of the galaxy was found to be insensitive to the exact binwidth chosen (2048 or 4096). The spectra were then filtered in order to eliminate both the low frequency spurious components left by the subtracted continuum, and the high frequency binning noise. The best set of filter parameters was chosen to maximize the significance of the CCF. The peak of the CCF was fit by a quadratic polynomial, determining both the wavelength shift, from its position, and the error, from its width.

#### 4.1 Template Spectra

During the course of the project, 27 templates were observed, 17 at ESO and 10 at the AAT. Fifteen of the ESO templates were galaxies, some of which were late-type galaxies with very accurate 21cm line redshifts (errors  $\sim 10 \text{ km s}^{-1}$ , da Costa *et al.* 1984). These were used to set the zero point for the whole set of templates. The other 2 ESO templates were radial velocity standard stars of spectral type K, taken from the Astronomical Almanac. The AUTOFIB templates were all standard stars from the Astronomical Almanac, however these were discarded as the ESO templates were of a higher quality. To check the zero-point reliability of the templates, they were cross-correlated against each other (including the 21cm galaxies), to obtain the redshift of each template with respect to the other 16. For each object, the difference between its published redshift and the measured redshifts from the other 16 templates was calculated. Overall, seven of the original seventeen ESO templates were classified as having very reliable zero-points, and selected to be used in the cross-correlation technique. Two more archive templates were chosen on the basis of their previous reliability and high signal-to-noise (Parker, Beard, & MacGillivray 1987). Finally, we chose as a further template, the high signal-to-noise spectrum of a galaxy in A4038. This was meant to provide at least one potentially good AAT template. In reality, the ESO templates proved to be superior, with no visible systematic effect. The ten final templates are listed in Table 1 along with their published redshifts.

#### 4.2 Cross-Correlation and Errors

The major advantage of the cross-correlation technique is that it preserves the statistical information on the redshift contained in the whole spectrum. A useful feature of the cross-correlation package used was the ability to place a confidence level on the chosen CCF peak by comparing its height with that expected for a random noise peak in the CCF. This followed the Tonry & Davis prescription (see Heavens 1993 for a new, more accurate approach to the problem). We introduced into the cross-correlation program a confidence level estimate on the redshifts obtained, based on the stability of the result provided by the different templates. Each galaxy spectrum was cross-correlated against the 10 templates described above and a confidence level was assigned to each cross-correlation. Spectra with 5 or more templates in agreement (within the errors on the redshifts) with confidence levels above 0.95 ( $\simeq 2\sigma$ ) were passed as secure. Spectra that did not satisfy these criteria were inspected by eye. Most of these spectra had between 2 and 4 templates in agreement and the visual inspection often supported this lower level of agreement. Spectra were discarded if there was no agreement between the templates and a visual inspection could not determine the redshift. Once a spectrum had been accepted as secure (visually or with  $\geq 5$  templates), the template redshift with the highest confidence level was assigned to the galaxy. If several templates had the same confidence, then the one with the lowest returned internal error was used. For high signal-to-noise spectra, it was common to find all the templates agreeing to within with a scatter of  $\Delta v \simeq 50 \text{ km s}^{-1}$ . Lower signal-to-noise spectra

had a typical scatter of  $\Delta v \simeq 100 \text{ km s}^{-1}$ . A small fraction of the galaxies had emission lines in their spectra. However, in most cases the emission lines did not provide redshifts of sufficient accuracy ( $\delta v \simeq 250 \text{ km s}^{-1}$ ) and these were only used when no absorption redshift was available.

Following the prescription of Tonry & Davis (1979), the cross-correlation programme provides an estimate of the internal error on the redshift, based on the width of the cross-correlation peak. For our data this ranged between  $14 \text{ km s}^{-1}$  and  $683 \text{ km s}^{-1}$ .

Throughout the course of the project, a total of 30 galaxy redshifts were repeated. These repeat observations can be used to provide an estimate of the external error on the redshifts. Table 2 shows the redshifts for all the repeat measurements in the survey along with the telescope on which each redshift was measured. The median offset between all these repeats is  $\simeq 200 \text{ km s}^{-1}$ , implying an *rms* external error of  $\simeq 140 \text{ km s}^{-1}$ . This value is representative of the error on all three telescopes on which the redshifts were measured. In Table 3 we present all the galaxy redshifts obtained in each cluster field as part of the EM survey.

## 5 CLUSTER REDSHIFTS

### 5.1 Determining Cluster Membership

The redshift of a cluster was defined in an objective manner which removed any subjective “eyeball” determination of whether a galaxy was in a cluster or not and provided a set of well-defined selection criteria that could be accurately reproduced. In addition, these criteria were used to quantify the contamination due to galaxy interlopers and used to determine the frequency of phantom clusters. We first experimented with the simple  $3\sigma$  pessimistic clipping scheme adopted by Colless & Hewett (1987). This method worked well for most cases to remove single outliers but broke down in cases where the clusters had a significant fraction of galaxies away from the main concentration (e.g. E519). We therefore supplemented the clipping algorithm with criteria similar to those described by Struble & Rood (1991b), which can be outlined as follows:

- (i) The mean and standard deviation of all the galaxy redshift measurements for a single cluster were calculated. The most discrepant galaxy redshift was temporarily removed from the galaxy listing and the mean redshift and standard deviation ( $\sigma_r$ ) were re-calculated. If  $\sigma_r$  was found to be outside the range  $\sigma_f < \sigma_r < 4\sigma_f$ , where  $\sigma_f$  ( $= 700 \text{ km s}^{-1}$ ) is a fiducial median cluster velocity dispersion, as quoted by Zabludoff, Huchra & Geller (1990), then it was set to the nearest of these limits to take account of clusters with unrealistically large or small values of  $\sigma_r$ .
- (ii) All the galaxy redshifts taken for a particular cluster were binned in redshift with a binwidth equal to  $\sigma_f$ .
- (iii) The cluster redshift distribution was searched for its highest peak. Once found, other peaks in its vicinity were located and merged if they were  $< \sigma_r$  away from the original peak. Various multiples of  $\sigma_r$  were tried, but it was found empirically that a threshold of  $\sigma_r$  gave the most realistic results. All the galaxy redshift measurements that had been merged into this one peak were

written out and removed from the galaxy listing. This procedure was repeated until all the redshift peaks had been located, which produced a list of redshift concentrations for the cluster which could vary from a single galaxy to all the galaxies observed in that cluster.

- (iv) For each concentration, the mean redshift and the fraction of observed galaxies within that concentration were calculated. The concentration with the highest fraction was taken as representative of the true cluster redshift.
- (v) If a cluster had a secondary concentration within its distribution that contained more than a third of the observed galaxies and was separated by more than  $1500 \text{ km s}^{-1}$  *i.e.*  $\simeq 2$  binwidths, from the largest concentration mentioned above, then the cluster was defined as a projection effect or phantom cluster. If the peaks were separated by less than  $1500 \text{ km s}^{-1}$ , then they were merged together and re-analysed (Stage 4). This guarded against clusters with subclustering and/or high velocity dispersions being broken up and classed as spurious. All the remaining redshift concentrations for a cluster were defined as interlopers. These values of acceptance were found empirically.

If the number of residual galaxies left in a cluster after  $3\sigma$  clipping was more than 2 larger than the results of the de-projection, then the latter result was adopted. For clusters with fewer than 5 members, only obvious outliers were removed, as the statistics on  $\sigma_r$  were then too poor. The above algorithm is rather crude and in all probability could be improved. For example, by weighting each galaxy redshift by the inverse of the distance from the cluster centroid or using the distribution of apparent magnitudes for the galaxies (see Dalton *et al.* 1994). A notable example where our criteria may be too rigid is E127 (Abell 3856) which we class as a projection effect (fig. 2). It was observed at the AAT and thus has measured galaxies distributed over the 40 arcmin AUTOFIB field-of-view. The two galaxies within the cluster core plus another two more external ones share a similar redshift of  $\sim 40000 \text{ km s}^{-1}$ , thus suggesting that value as the possible cluster redshift. The mean cluster velocity and standard error for all EM clusters are shown in Table 4.

### 5.2 Interlopers and Phantom Clusters

The objective criteria described above lead to a natural definition of an interloper and a phantom cluster and provide direct estimates of the contaminating percentages in the EDCC. To do this we confine ourselves to the ESO data only, since the smaller field-of-view constrains the observations to the cluster cores. For all the observed ESO EM clusters, the percentage of clusters that had any amount of interloper contamination is 65%. For these clusters, but excluding phantom ones, the percentage of sampled redshifts per cluster defined as interlopers is 27%. The number of spurious clusters (30% of members more than  $1500 \text{ km s}^{-1}$  away) out of the total 83 EM clusters observed at ESO is 8, *i.e.* 10%. For the small-Abell-radius sample used in Nichol *et al.* (1992), 6 clusters were classified as phantom *i.e.* 6% of that sample. These figures indicate that a single redshift taken towards the core of a cluster has a significant chance of not being a member of that cluster. In addition,  $\sim 10\%$  of

rich clusters selected in projection on the sky seem to have a richness which is overestimated by  $\sim 30\%$ .

It is interesting to compare these figures with those obtained for the Abell catalogue which rely on detailed modelling techniques. Our results are in reasonable agreement with Lucey (1983), who uses Monte Carlo simulations to estimate that 15% – 25% of Abell clusters are significantly contaminated ( $\geq 50\%$ ). The value of  $\simeq 50\%$  estimated from an analytical models by Fesenko (1979) is significantly higher than our estimates. Struble & Rood (1991b) used redshift measurements to estimate that only 3% – 5% of Abell clusters were superpositions and thus spurious. Our data would suggest that this is an under-estimate. Their low value might be due to the fact that they were mainly concerned with estimating the effects of interloper contamination on the richness of the cluster and whether a cluster could be boosted up into Abell’s statistical sample. Therefore, they set out with the apriori assumption that all the “clusters” are clusters of some form or another, so their result is probably a lower limit.

### 5.3 Cluster Redshift Comparisons

Our data can be compared with several recent compilations of cluster redshifts. A total of 13 clusters are common with the recently published APM list of cluster redshifts based on 2 galaxies per cluster and a likelihood estimator (Dalton *et al.* 1994). Of these, 12 have an absolute average median velocity residual of  $295 \text{ km s}^{-1}$  (E261, E400, E410, E447, E462, E557, E683, E699, E735, E742, E748, E765). For one cluster the difference in methodology between many redshifts per cluster and a likelihood estimator to determine cluster redshifts becomes more apparent. For the cluster, E470, our redshift, based on 7 galaxies, is  $32903 \text{ km s}^{-1}$ . Dalton *et al.* adopt a cluster redshift from their single measured galaxy redshift of  $22784 \text{ km s}^{-1}$ , rather than their likelihood value of  $32647 \text{ km s}^{-1}$ , which is in fact much closer to our value. There are 3 clusters in common with the clusters observed by Colless & Hewett (1987). The clusters E124, E394 and E400 have redshift differences (EDCC-C&H) of  $-547 \text{ km s}^{-1}$ ,  $-45 \text{ km s}^{-1}$  and  $-334 \text{ km s}^{-1}$  respectively. E400 has also been observed extensively by Teague, Carter & Gray (1990) who have measured the redshifts of 72 cluster members. There is a difference in these redshift estimates (EDCC-T&G) of  $145 \text{ km s}^{-1}$ . The recent compilation of Abell redshifts published by Lauer & Postman (1994) has 4 clusters in common with our own. The clusters E348 and E394 have velocity differences (EDCC-L&P) of  $258 \text{ km s}^{-1}$  and  $-28 \text{ km s}^{-1}$  respectively. For the cluster E372 we have only one redshift of  $12675 \text{ km s}^{-1}$  for a galaxy located 4 arcmins from the Abell cluster centre. Lauer & Postman (1994) quote a redshift of  $14739 \text{ km s}^{-1}$  for this cluster. There is a larger discrepancy between the measured redshifts of E557. Lauer & Postman (1994) quote a redshift for this cluster (A2911) of  $6074 \text{ km s}^{-1}$ . We have taken redshifts for 8 galaxies towards this cluster and 6 have a mean of  $23729 \text{ km s}^{-1}$  with a small velocity dispersion of  $413 \text{ km s}^{-1}$ . This result is almost midway between the Dalton *et al.* (1994) measured redshifts of  $23174 \text{ km s}^{-1}$  and  $24193 \text{ km s}^{-1}$ . Fig. 3 shows a right ascension cone diagram of all the EM clusters classified as genuine, including the lit-

erature clusters, providing a view of how these systems delineate the large-scale structure of the universe. The details of this distribution, and particularly the comparison with previous results from galaxy redshift surveys, have been discussed elsewhere (Guzzo *et al.* 1992, Nichol *et al.* 1992).

## 6 VELOCITY DISPERSIONS

### 6.1 Estimator and Results

The line-of-sight velocity dispersions have been estimated for all clusters in the sample which have 6 or more redshifts belonging to the cluster, on the above definition. The velocity dispersions have been calculated using the rigorous procedure described by Danese, De Zotti & di Tullio (1980). The radial velocity dispersion  $\sigma_v$  is given by

$$\sigma_v = \sum_{i=1}^N v_i^2 / (n - 1) - \delta^2 / (1 + \bar{V})^2, \quad (1)$$

where  $\bar{V}$  is the mean cluster redshift ( $\bar{V} \simeq c\bar{z}$ ),  $\delta$  is the contribution from the measurement error, and  $v$  is line-of-sight component of the velocity of a galaxy with respect to the cluster centre, given by

$$v = (V - \bar{V}) / (1 + \bar{V}/c), \quad (2)$$

where  $V \simeq cz$  is the redshift of each galaxy. We have also calculated the statistical uncertainty in the velocity dispersions using the prescription given in Danese *et al.* (1980). This accurately takes into account sampling errors, experimental errors and cosmological corrections. The values of  $\sigma_v$  and their errors for 37 EDCC clusters with a net number of galaxies per cluster  $N_{clus} \geq 6$  are presented in Table 4.

There are three of our clusters in common with the Colless & Hewett (1987) sample of cluster velocity dispersions for which they have  $N_{clus} \simeq 40$ . The velocity dispersion differences (EDCC-C&H) for the 3 clusters E124, E394, E400 are  $-169 \text{ km s}^{-1}$ ,  $51 \text{ km s}^{-1}$  and  $211 \text{ km s}^{-1}$  respectively. Teague *et al.* (1990) find  $\sigma_v = 885 \text{ km s}^{-1}$  for E400 using  $N_{clus} \simeq 70$  galaxies. This is  $\simeq 1.5 \sigma$  smaller than our estimate of  $1222 \text{ km s}^{-1}$  based on 7 galaxies.

### 6.2 Comparison with Cosmological Models

The velocity dispersions of clusters can be used to place conservative constraints on cosmological models. Frenk *et al.* (1990) (hereafter FWED) calculate the distribution of velocity dispersions for  $R \geq 1$  clusters in several  $\Omega = 1$  cold dark matter (CDM) cosmologies with different values for the biasing parameter  $b$ . In comparing our data with FWED, we follow closely the procedure of Zabludoff *et al.* (1990) and compare two statistics; the largest expected velocity dispersion in our sample and the median velocity dispersion of the whole sample. FWED present the velocity distributions for clusters selected from simulations carried out in 3-D (their Fig. 1). In addition, they argue that projection can seriously contaminate cluster selection leading to an over-estimate of the velocity dispersions. Therefore, they also model cluster selection in 2-D by subjecting cluster catalogues from the simulations to projection effects expected in the Abell catalogue and using techniques employed in the analysis of real clusters (their Fig. 3).

A histogram of the velocity dispersions for our sample of 37 clusters is shown in Fig. 4. The largest velocity dispersion in our sample of 36 is E400 (A2721) with  $\sigma_v = 1222^{+606}_{-243} \text{ km s}^{-1}$ . However, the comparison with the more accurate measurement of Teague, Carter & Gray (1990) reported in section 6.1, indicates this to be overestimated by  $\sim 350 \text{ km s}^{-1}$ . The next highest is E606 (Abell 2962), with  $\sigma_v = 1152^{+377}_{-190} \text{ km s}^{-1}$ . Interestingly, these values are not a good fit to the Frenk *et al.* 2-D velocity dispersion model, which predicts too many clusters with high velocity dispersions ( $\geq 25\%$  with  $\sigma_v \geq 1200 \text{ km s}^{-1}$  for  $b \leq 2.5$ ). Comparing with the 3-D selection predictions, the only compatible CDM models are those with  $b \geq 1.6$ , which predict  $\leq 10\%$  of clusters will have  $\sigma_v \geq 1200 \text{ km s}^{-1}$ . For  $b = 1.3$  the predicted fraction rises to 40% and can be ruled out.

In order to compare the median velocities of our sample with the predictions of CDM for  $R \geq 1$  clusters we construct a sub-sample of 24 clusters which satisfy the criteria  $R \geq 1$ . For these clusters we derive a median cluster velocity dispersion of  $742 \pm 63 \text{ km s}^{-1}$ . This agrees to within  $1\sigma$  with the predictions of the median velocities for CDM with  $b = 1.6 - 2.0$ , viz.  $850 \text{ km s}^{-1}$  and  $760 \text{ km s}^{-1}$  respectively (Zabludoff *et al.* 1990). For  $b \geq 2.5$  and  $b \geq 3.3$ , our value is too large by  $\geq 2\sigma$  and  $\geq 4\sigma$  respectively. If  $b \leq 1.3$ , then the predicted median velocity rises to  $\geq 1000 \text{ km s}^{-1}$  and is firmly inconsistent with the data.

In two independent comparisons the same conclusion can be reached; namely, the EM velocity dispersion data are most consistent with a  $b = 1.6$  or a  $b = 2.0$  CDM model and can strongly exclude models with  $b \geq 2.5$  and  $b \leq 1.3$ . These conclusions are in substantial agreement with those of Zabludoff *et al.* (1990) and Girardi *et al.* (1993), both of whom compare the distribution function of velocity dispersions for Abell cluster samples with the predictions of FWED. It should be taken into account, however, the possibility of a physical velocity bias which can lower the observed velocity dispersion in clusters to about 70% that of the dark matter. As shown by Couchman & Carlberg (1992), this would make a low bias ( $b=1$  or less) CDM model, compatible with the COBE-DMR measurements, to agree with basically all the current observational data, including those presented here.

## 7 THE CLUSTER-CLUSTER CORRELATION FUNCTION SAMPLE

One of the main motivations behind the construction of the EM survey was to re-estimate the cluster spatial auto-correlation function  $\xi_{cc}(r)$  from a sample where systematic errors and biases that had allegedly plagued previous estimates could be kept under control. As mentioned in Section 1, the major concern regarding the Abell catalogue was the extent to which it is seriously contaminated by projection effects. One of the easiest ways of reducing projection effects is to reduce the size of the counting radius within which the cluster is defined. This reduces the number of cluster overlaps and thus prevents the richness of distant clusters, which are in the haloes of nearby clusters, being overestimated and consequently being incorrectly included into the catalogue. In the construction of the Abell catalogue, a radius of  $1.5 h^{-1} \text{ Mpc}$  was used to define the clusters. Many

authors believe this is an overestimate for the size of clusters and even George Abell, in his original paper (Abell 1958), commented that his radius may be too large. The EDCC was constructed using the standard Abell radius mentioned above, as this allowed for a fair comparison between it and the Abell catalogue (Lumsden *et al.* 1992). However, for the above reasons, for the computation of the cluster correlation function a new sample of clusters was selected from the EDCC using a smaller radius of  $1.0 h^{-1} \text{ Mpc}$ . This reduced the number of deblended clusters from 30% in the standard EDCC to 8% in this sample (Nichol 1992). The final redshift sample used to calculate the correlation function discussed in Nichol *et al.* (1992) was thus selected using the following 3 criteria:

- (i) A background corrected  $m_{10}(b_j)$  of  $\leq 18.75$ , which corresponds to the completeness limit of the EDCC ( $z \sim 0.13$ ).
- (ii) Within the coordinate limits of  $21^{\text{h}}.88 < \text{RA} < 3^{\text{h}}.59$  and  $-42^{\circ}.40 < \text{Dec} < -22^{\circ}.88$ . This prevented clusters near the edge of the survey being included as their statistics were often uncertain.
- (iii) Clusters with a galaxy richness,  $R_1 \geq 22$  galaxy members within an Abell radius of  $1.0 h^{-1} \text{ Mpc}$ , after background correction.

From a comparison of the clusters in common between this sample and the Abell catalogue, the  $R_1 \geq 22$  richness cut corresponds to a richness cut of 40 for Abell clusters. This means that this small-Abell-radius sample of clusters is equivalent to a sample with richness cut between  $R = 0$  and  $R = 1$  Abell richness classes.

With the above richness threshold, 97 clusters were selected in total. These are listed in Table 5, along with the associated redshift information. Of these, 65 have redshifts from the EM survey, including 6 that were rejected as projection effects. A further 19 cluster redshifts are available from the literature and unpublished sources. These are also listed in Table 5. With the projection effects removed, the final redshift compilation has a completeness of 86% (78/91). Table 5 is almost identical to the cluster sample used for the correlation analysis (Nichol *et al.* 1992) although there are some differences. We have updated the list with new redshift information and re-classified E448 as a phantom cluster. In addition, clusters E450 and E297 were upgraded from phantom clusters to genuine cluster status on the basis of new data. For completeness, in Table 5 we include also the position angles and eccentricities derived for the clusters in Martin *et al.* (1995). The reader is directed to this paper for a full discussion of the methods used in deriving these values.

## 8 CONCLUSIONS

We present the redshifts of the galaxies and clusters which comprise the Edinburgh-Milano cluster redshift survey. The clusters in this work were selected from the digitised survey of the EDCC and  $\simeq 10$  redshifts have been secured in each cluster. The redshift data presented here for 94 clusters thus represent a large and homogeneous database. Using the galaxy redshifts we have developed an algorithm to exclude phantom clusters and interlopers from the survey.

About 10% of clusters in our survey are heavily contaminated confirming previous results that projection effects are a serious problem for optically selected rich clusters. This is the only digitised cluster survey to really attack the problem of projection effects by trying to de-project in 3-D. For 37 clusters we present line-of-sight velocity dispersions. From a comparison with structure formation models, the velocity dispersion data are most consistent with an  $\Omega = 1$  CDM model with a biasing parameter  $b = 1.6 - 2$  and are inconsistent with the model if  $2.5 \leq b \leq 1.3$ .

### Acknowledgments

We are indebted to the supporting staff of the European Southern Observatory and the Anglo-Australian Observatory for their excellent assistance during the observations of this project. We also would like to thank N. Heydon-Dumbleton for his important contribution to the starting of this project, and J. Huchra, H. Andernach, A. Broadbent, D. Nicholson, D. Lambas, Q. Parker, J. Peacock, T. Shanks for providing both published and unpublished redshifts. Heinz Andernach is warmly acknowledged for useful suggestions to a draft of this paper. CAC acknowledges the SERC for the award of an Advanced Fellowship and RCN also acknowledges the SERC for receipt of a studentship and travel grants. This work has received partial financial support from the European Community (EEC contract ERB-CHR-XCT-920033).

### REFERENCES

- Abell, G.O., 1958, *ApJS*, 3, 211  
 Abell, G.O., Corwin, H.G., Olowin, R.P., 1989, *ApJ*, 70, 1  
 Bahcall, N.A., Soneira, R.M., 1983, *ApJ*, 262, 20  
 Borgani, S., Plionis, M., Coles, P., Moscardini, L., 1995, *MNRAS*, in press  
 Ciardullo, R., Ford, H., Harms, R., 1985, *ApJ*, 293, 69  
 Colless, M.M., Hewett, P., 1987, *MNRAS*, 224, 453  
 Couchman, H.M.P., Carlberg, R.G., 1992, *ApJ*, 389, 453  
 Croft, R.A.C., Efstathiou, G., 1994, *MNRAS*, 267, 390  
 da Costa, L.N., Pellegrini, P.S., Nunes, M.A., Willmer, C., Latham, D.W., 1984, *AJ*, 89, 1310  
 Dalton, G.B., Efstathiou, G., Maddox, S.J., Sutherland, W.J., 1994, *MNRAS*, 269, 151  
 Danese, L., De Zotti, G., di Tullio, G., 1980, *A&A*, 82, 322  
 Dekel, A., Blumenthal, G.R., Primack, J.R., Olivier, S., 1989, *ApJ*, 338, L5  
 Efstathiou, G., Dalton, G.B., Sutherland, W., Maddox, S.J., 1992, *MNRAS*, 257, 125  
 Ellis, R.S., Parry, I.R., 1988, in "The Ninth Santa Cruz Summer Workshop in Astronomy and Astrophysics: Instrumentation for Ground-Based Optical Astronomy, Present and Future", Robinson L.B. ed., Springer-Verlag, New York, p. 192  
 Etori, S., Guzzo, L., Tarengi, M., 1995, submitted to *MNRAS*  
 Fesenko, B.I., 1979, *Soviet Astronomy*, 23, 6  
 Frenk, C.S., White, S.D., Efstathiou, G., Davis, M., 1990, *ApJ*, 351, 10  
 Girardi, M., Biviano, A., Giuricin, G., Mardirossian, F., Mezzetti, M., 1993, *ApJ*, 404, 38  
 Guzzo, L., Collins, C.A., Nichol, R.C., Lumsden, S.L., 1992, *ApJ*, 393, L5  
 Heavens, A.F., 1993, *MNRAS*, 263, 735  
 Heydon-Dumbleton, N.H., Collins, C.A., MacGillivray, H.T., 1989, *MNRAS*, 238, 379  
 Huchra, J.P., Geller, M.J., Clements, C.M., Tokarz, S.P., Michel, A., 1992, (*Z cat.*)

- Lauer, T.R., Postman, M., 1994, *ApJ*, 425, 418  
 Lissandrini, C., Cristiani, S., La Franca, F., 1994, *PASP*, 106, 1157  
 Loveday, J., 1991, Ph.D. Thesis, University of Cambridge  
 Lucey, J.R., 1983, *MNRAS*, 204, 33  
 Lumsden, S.L., Nichol, R.C., Collins, C.A., Guzzo, L., 1992, *MNRAS*, 258, 1  
 Maddox, S.J., Efstathiou, G., Sutherland, W.J., 1990, *MNRAS*, 246, 433  
 Mann, R., Heavens, A.F., Peacock, J.A., 1993, *MNRAS*, 263, 798  
 Martin, D.R., Nichol, R.C., Collins, C.A., Lumsden, S.L., Guzzo, L., 1995, *MNRAS*, in press  
 Muriel, H., Nicotra, M., Lambas, D.G., 1990, *AJ*, 100, 339  
 Muriel, H., Nicotra, M., Lambas, D.G., 1991, *AJ*, 101, 1997  
 Nichol, R.C., 1992, Ph.D. Thesis, University of Edinburgh  
 Nichol, R.C., Collins, C.A., Guzzo, L., Lumsden, S.L., 1992, *MNRAS*, 255, 21p  
 Nicholson, D., 1991, Ph.D. Thesis, University of Edinburgh  
 Olowin, R., de Souza, R.E., Chincarini, G., 1988, *A & AS*, 73, 125  
 Parker, Q.A., Beard, S.M., MacGillivray, H.T., 1987, *A & A*, 173, L5  
 Parry, I.R., Sharples, R.M., 1988, in *ASP Conf. Ser.*, Vol. 3, "Fibre optics in astronomy", Barden, S.C. ed., *Astron. Soc. Pac.*, San Francisco, p. 93  
 Peacock, J.P., West, M.J., 1992, *MNRAS*, 259, 494  
 Peterson, B.A., Ellis, R.S., Efstathiou, G., Shanks, T., Bean, A.J., Fong, R., Zen-Long, Z., 1986, *MNRAS*, 221, 233  
 Postman, M., Huchra, J.P., Geller, M.J., 1992, *ApJ*, 384, 404  
 Struble, M.F., Rood, H.J., 1991a, *ApJS*, 77, 363  
 Struble, M.F., Rood, H.J., 1991b, *ApJ*, 374, 395  
 Sutherland, W., 1988, *MNRAS*, 234, 159  
 Tonry, J., Davis, M., 1979, *AJ*, 84, 1511  
 Teague, P., Carter, D., Gray, P.M., 1990, *ApJS*, 72, 715  
 Zabludoff, A.I., Huchra, J.P., Geller, M.J., 1990, *ApJS*, 74, 1

**Figure 1.** Example of a good S/N galaxy spectrum observed with EFOSC and the 3.6 m ESO telescope.

**Figure 2.** Four examples of observed clusters, chosen to show both the results of using different instrumentation and the differences in the degree of foreground/background contamination. The sky plots (left panels for E460 and E495) have a size which corresponds to the angular Abell radius of the cluster. The size of the circles is proportional to the  $b_j$  magnitude of the galaxies (extracted from the EDSGC), with the small dots representing objects fainter than  $b_j = 19.5$ , and the largest circles (in the left panel) corresponding to galaxies brighter than  $b_j = 15$ . The crosses mark the objects for which a redshift appears in Table 3. E127 and E712 have been observed only at the AAT — using AUTOFIB — as indicated by the sparse distribution of the crosses: E127 is a case classified as projection on the basis of the available redshifts. E460 has been observed both at ESO and at the AAT, while E495 at ESO only. For these two cases, the bulk of redshifts is concentrated in the center of the cluster core, due to the small field of EFOSC. This region (dashed square) is zoomed in the right panel for more clarity.

**Figure 3.** Right ascension cone diagram for both the EM cluster redshifts and those found in the literature for the small-Abell-radius sample of Table 5. The declination slice runs from  $-42^\circ.5 \leq \text{Dec} \leq -22^\circ.5$

**Figure 4.** The distribution of velocity dispersions for a sample of 37 EM clusters with  $N_{\text{clus}} \geq 6$ .

Name	RA	DEC	$m_B$	$cz$
N5740	14 41 53	01 53	12.5	$1575 \pm 20$
N5746	14 42 23	02 10	11.5	$1801 \pm 33$
N5921	15 19 30	05 15	12.0	$1480 \pm 10$
N6070	16 07 24	00 50	12.5	$2005 \pm 7$
N6118	16 19 12	-02 10	12.0	$1578 \pm 15$
N6958	20 45 30	-38 11	12.2	$2742 \pm 50$
N7793	23 57 48	-32 35	9.1	$231 \pm 7$
A4038	23 45 08	-28 25	13.7	$8813 \pm 65$
HD171391	18 34 37	10 59	5.1	$6.9 \pm 0.2$
HD35410	05 21 56	-00 56	5.2	$20.5 \pm 1.0$

Table 1: Characteristics of the 10 templates used with the cross-correlation routine. The last two are stellar spectra (from Parker *et al.* 1987). The others are new galaxy templates specifically observed during the survey. Literature heliocentric redshifts, in  $\text{km s}^{-1}$ , are from Da Costa *et al.* (1984).